AD-A031 389 WEIDLINGER ASSOCIATES NEW YORK F/G 8/13
CALCULATIONS OF THREE TEST PROBLEMS BY THE 3-D TRANAL CODE.(U)
APR 76 J P WRIGHT, J L BAYLOR DNA001-74-C-0219
UNCLASSIFIED DNA-3998F NL

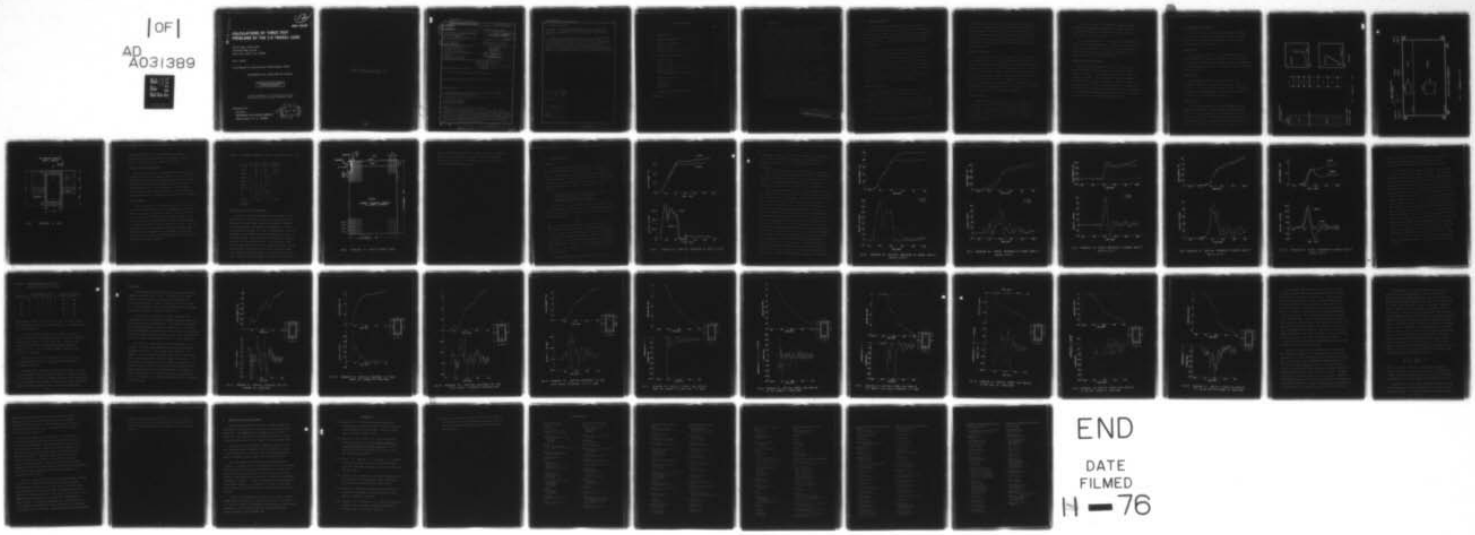

END
DATE FILMED
H-76

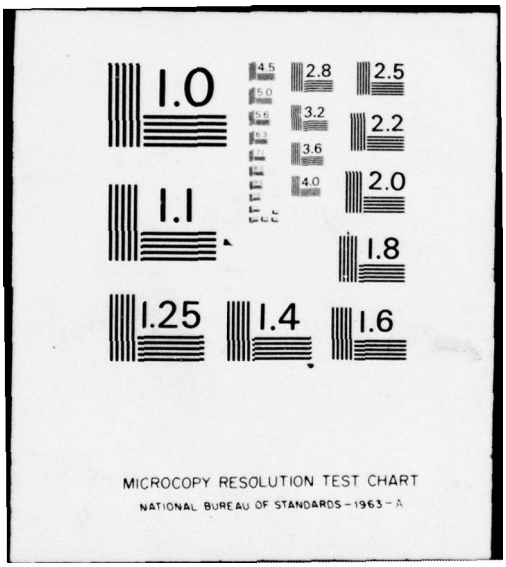
1.0
1.1
1.25
1.4
1.6
1.8
2.0
2.2
2.5
2.8
3.2
3.6
4.0
4.5
5.0
MICROCOPY RESOLUTION TEST CHART
NATIONAL BUREAU OF STANDARDS-1963-A

12

DNA 3998F

CALCULATIONS OF THREE TEST PROBLEMS BY THE 3-D TRANAL CODE

Weidlinger Associates
110 East 59th Street
New York, New York 10022

April 1976

Final Report for Period April 1974—March 1976

CONTRACT No. DNA 001-74-C-0219

THIS WORK SPONSORED BY THE DEFENSE NUCLEAR AGENCY
UNDER RDT&E RMSS CODE B344076464 Y99QAXSC06144 H2590D.

Prepared for
Director
DEFENSE NUCLEAR AGENCY
Washington, D. C. 20305

Destroy this report when it is no longer needed. Do not return to sender.

UNCLASSIFIED

SECURITY CLASSIFICATION OF THIS PAGE (When Data Entered)

REPORT DOCUMENTATION PAGE

READ INSTRUCTIONS BEFORE COMPLETING FORM

1. REPORT NUMBER: DNA 3998F
2. GOVT ACCESSION NO.
3. RECIPIENT'S CATALOG NUMBER
4. TITLE (and Subtitle): CALCULATIONS OF THREE TEST PROBLEMS BY THE 3-D TRANAL CODE,
5. TYPE OF REPORT & PERIOD COVERED: Final Report for Period April 1974—March 1976
6. PERFORMING ORG. REPORT NUMBER
7. AUTHOR(s): Joseph P. Wright, John L. Baylor
8. CONTRACT OR GRANT NUMBER(s): DNA 001-74-C-0219
9. PERFORMING ORGANIZATION NAME AND ADDRESS: Weidlinger Associates, 110 East 59th Street, New York, New York 10022
10. PROGRAM ELEMENT, PROJECT, TASK AREA & WORK UNIT NUMBERS: NWED Subtask Y99QAXSC061-44
11. CONTROLLING OFFICE NAME AND ADDRESS: Director, Defense Nuclear Agency, Washington, D.C. 20305
12. REPORT DATE: April 1976
13. NUMBER OF PAGES: 50
14. MONITORING AGENCY NAME & ADDRESS (if different from Controlling Office): 43 p.
15. SECURITY CLASS (of this report): UNCLASSIFIED
15a. DECLASSIFICATION/DOWNGRADING SCHEDULE

16. DISTRIBUTION STATEMENT (of this Report)

Approved for public release; distribution unlimited.

17. DISTRIBUTION STATEMENT (of the abstract entered in Block 20, if different from Report)

18. SUPPLEMENTARY NOTES

This work sponsored by the Defense Nuclear Agency under RDT&E RMSS Code B344076464 Y99QAXSC06144 H2590D.

19. KEY WORDS (Continue on reverse side if necessary and identify by block number)

Soil-Structure Interaction
Structural Vulnerability
TRANAL Computer Program

20. ABSTRACT (Continue on reverse side if necessary and identify by block number)

TRANAL, a three-dimensional, finite element, transient nonlinear analysis code, was used to calculate a series of three simple test problems. Although the test problems are not three-dimensional, a number of different aspects of the code were checked including timing, data management, nonlinear cap model routine, applied air pressure routine (Brode fit), and mesh generation. The test problems were designed by the Space and Missile Systems Organization in conjunction with TRW personnel.

NEXT PAGE

DD FORM 1 JAN 73 1473 EDITION OF 1 NOV 65 IS OBSOLETE

UNCLASSIFIED

SECURITY CLASSIFICATION OF THIS PAGE (When Data Entered)

373050

20. ABSTRACT (Continued)

For two of the problems, TRANAL results are compared with results from LAYER, a two-dimensional, axisymmetric, finite difference code. The results compare quite well when the differences in code details are considered.

A third problem, which involves a hollow concrete cylinder embedded in a two-layer soil system (clay over shale), is also studied. The conclusion reached is that, for the prescribed airblast loading (nuclear type), the walls of the cylinder will not fail in compression during the first 100 milliseconds, which is probably the most critical period. However, this conclusion is based on a simple two-dimensional, axisymmetric problem; in order to understand this soil-structure interaction problem more fully, it is necessary to perform a complete three-dimensional analysis.

TABLE OF CONTENTS

I INTRODUCTION

During the last ten years, there has been considerable progress in the development of computer codes for three dimensional, transient, nonlinear analysis of soils and structures, Refs. [1] and [2]. Such codes can be used to study structural problems which are of interest in both civilian and military applications. A defense problem of much interest is the vulnerability of protective structures to high explosive and nuclear weapons. In particular, the vulnerability of underground missile silos is of primary concern to the United States Air Force (USAF).

The TRANAL code, Ref. [3], was developed by Weidlinger Associates (WA) under a previous Defense Nuclear Agency (DNA) contract with vulnerability problems in mind. In order to check certain capabilities of TRANAL, a series of three simple test problems were calculated. These three problems, which were designed by the Space and Missile Systems Organization (SAMSO) in conjunction with TRW personnel, were run as part of the current DNA contract and the results are reported herein. Some TRANAL - related code developments are also discussed.

II TRANAL DEVELOPMENTS

Although the basic TRANAL code has been operational since September 1974, there have been subsequent developments which are worth noting. These relate to graphics capability, data generation techniques, improvements in execution speed and more flexibility in its use for vulnerability problems for the USAF.

In order to run a large 3-D problem, it is frequently necessary to prepare a great deal of data before making a run. In a problem with complicated geometry and several different materials, it is not uncommon to prepare more than 10,000 data items. The preparation of such large amounts of data is usually an error prone task and various techniques are needed to reduce errors and speed data preparation. As a result, graphics capability and a data input aid, called region preprocessing, have been added to TRANAL.

Region Preprocessing

As outlined in Ref. [2], TRANAL is designed to use a technique referred to as zone processing in which a structural complex is subdivided into a set of substructures, called zones, and each zone is further subdivided into a set of elements. This two-level hierarchical procedure is used so that each substructure will fit into computer memory during the main calculational phase.

An extension of TRANAL which is referred to as region

preprocessing is now operational. Each zone is subdivided into a set of regions which can be further subdivided into sets of elements. A region is a set of elements which all have the same material type. This three-level hierarchical procedure is used only during the data input phase of the calculation. Zone processing is still employed during the calculational phase.

Graphics Capability

The capability now exists to make plots of the elements in each zone, or of the regions defined in the problem set up. Thus, the coordinates and material layout produced by mappings and mesh generators can be viewed in order to check problem set up. The plotting routines used were obtained from library programs in the public domain. The main work was the adaptation of these routines to use the TRANAL data structures which are complicated by zone processing. Additional plotting capability for viewing results will be developed in the future when the need arises in a particular application.

Execution Speed

TRANAL is currently operational on the CDC 6600 at New York University and on the CDC 7600 at Lawrence Berkeley Laboratory. Execution speed is less than 0.5 milliseconds per element per time step on the 7600; this includes the latest CAP model routine, Ref. [4], and all overhead due to data management.

At the current rate, a calculation requiring 10,000 elements and 1,000 time steps would cost about $1,500.00 (1½ hours of 7600 time) and could be expected to run overnight once the problem is set up.

In a recent preliminary calculation for the HARD PAN I-3 event, a full three dimensional calculation was made with 6156 elements (21,840 degrees of freedom) for 660 time steps. This calculation required 32 minutes of CDC 7600 time and cost $440.00 at the overnight rate (80%).

SAMSO Vulnerability Problems

Missile silo vulnerability studies are conducted by using an applied air blast loading to simulate a nearby nuclear explosion. Two air blast loading routines are now available in TRANAL. Both loadings are based on Brode's fits, Ref. [5], to a nuclear air burst. These two fits are the Brode direct fit and the Brode simple fit. In addition, two data generators have been built especially for the geometry of the missile silo vulnerability problem in order to reduce time and errors in the data generation process.

III SAMSO-TRW TEST PROBLEMS

In order to check out certain capabilities of TRANAL, a series of three simple test problems, designed by SAMSO and TRW personnel, have been calculated. These problems are designated by P1, P2 and P3.

Problem 1 (P1)

This problem, called P1, is the one dimensional, plain strain response of a half-space of shale covered by 20 feet of clay which is subjected to a pressure history corresponding to a one megaton surface burst at the 600 psi peak overpressure location (see Fig. 1).

Problem 2 (P2)

This problem called P2, is the two dimensional, axisymmetric response of a half-space of shale covered by 20 feet of clay subjected to a pressure history corresponding to a one megaton surface burst in ranges between 2,000 psi and 200 psi peak overpressure (see Fig. 2).

Problem 3 (P3)

This problem called P3, is the two dimensional, axisymmetric response of a hollow concrete cylinder embedded in 20 feet of clay overlying a shale half-space (see Fig. 3). The cylinder, which is flush with the clay surface, is 40 feet in length, 10 feet in radius and has 4 feet thick walls on the top and bottom and 2 feet thick side walls. The

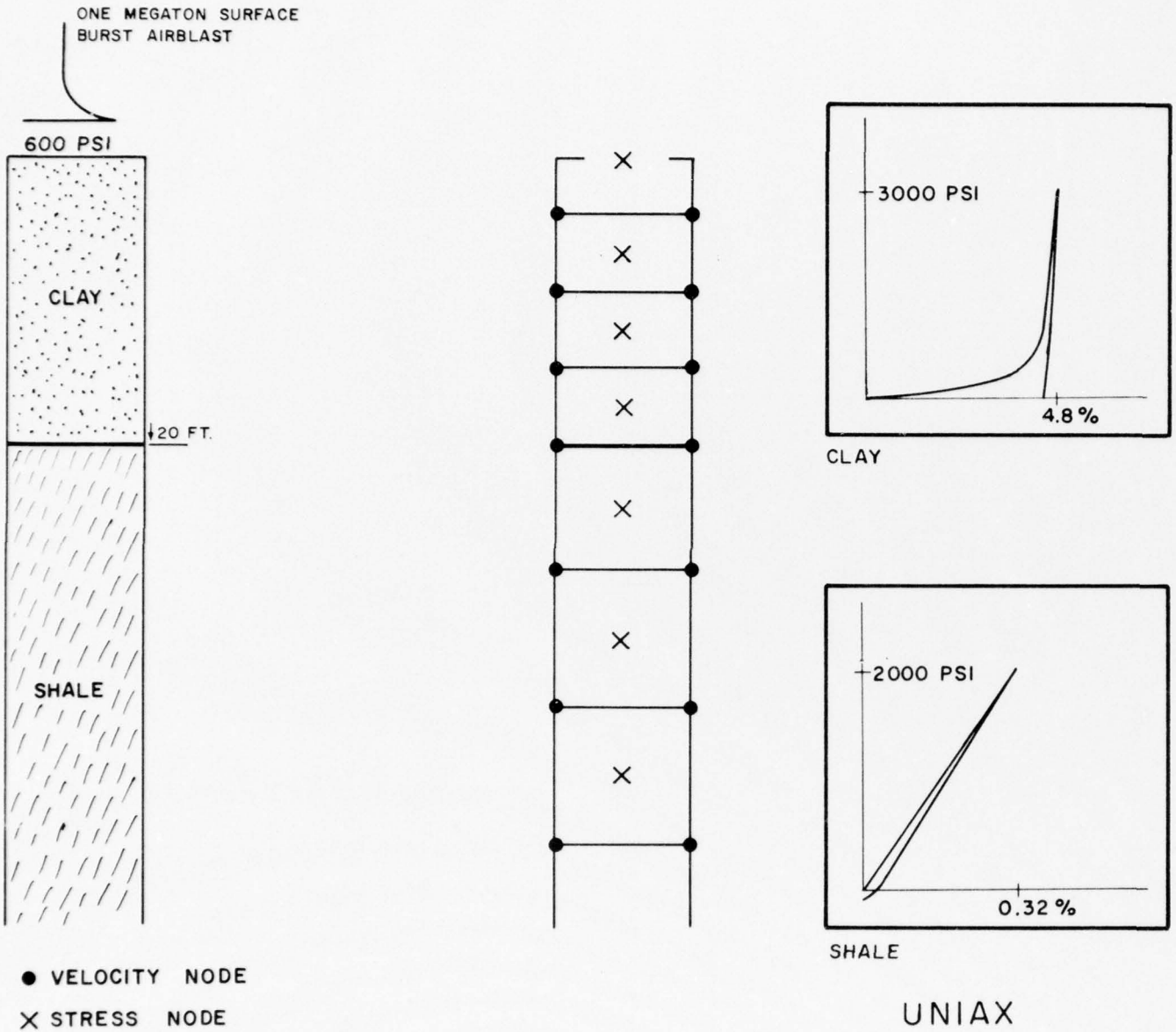

FIG. 1 PROBLEM 1 (P1)

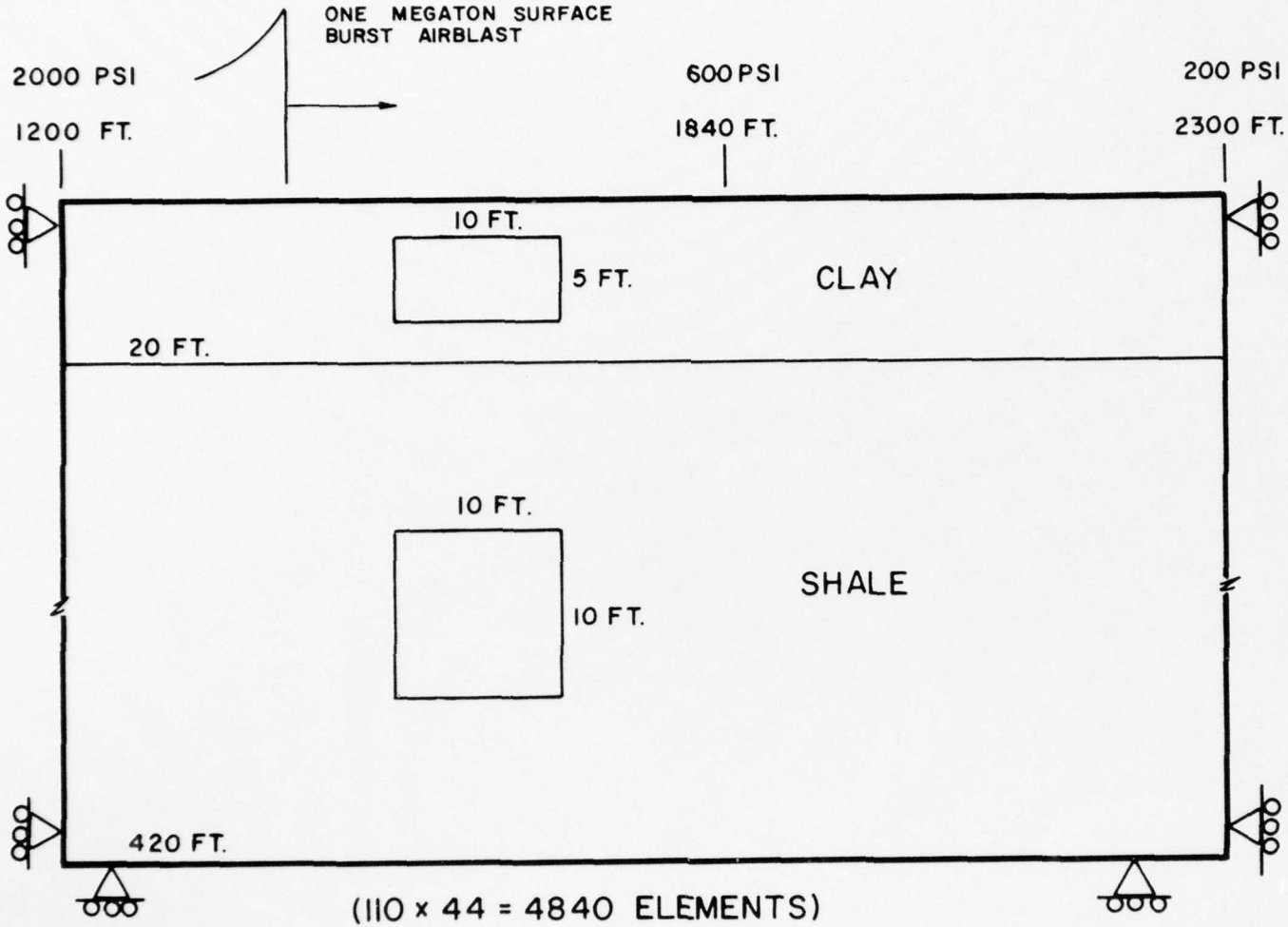

FIG. 2 PROBLEM 2 (P2)

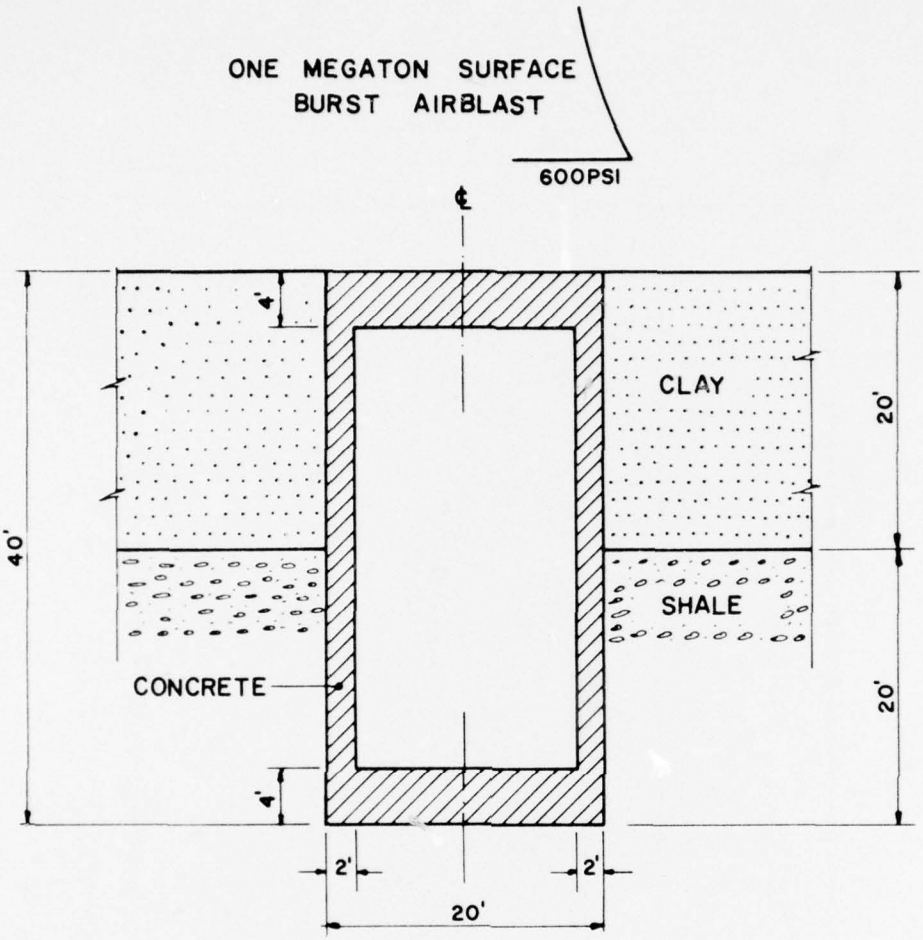

FIG. 3 PROBLEM 3 (P3)

clay/concrete surface is to be subjected everywhere to a pressure history corresponding to a one megaton surface burst at the 600 psi peak overpressure location.

Surface Pressure Time History

The pressure time history applied to the surface in all problems was based on the Brode simple fit, Ref. [5]. The response was calculated for 100 milliseconds after the time the 600 psi peak overpressure begins, which is roughly 108 milliseconds after the detonation of the one megaton surface burst. Thus, response curves for all calculations begin somewhat after 0.1 seconds and extend past 0.2 seconds.

Material Models

Material models for the clay and shale were represented by the soil CAP model, Ref. [6], in compression with mean stress, σ_m, limited in tension. Uniaxial compression curves for the clay and the shale are illustrated in Fig. 1. The concrete in P3 was represented by a linearly elastic model in compression with mean stress limited in tension. Since the stresses in the concrete never exceeded the assumed value of compressive failure (6,000 psi), this model is considered adequate for P3. Values of the parameters used for the three materials are given in Table I.

TABLE I. CAP MODEL PARAMETERS (Model as described in Ref. [6])

	Clay	Shale	Concrete
ρ(pcf)	120	137	150
K(ksi)	340	540	1600
G(ksi)	85	115	1250
A(ksi)	0.1	0.866	-
B(ksi^{-1})	1.5	2.5	-
C(ksi)	0.07	0.361	-
D(ksi^{-1})	2.0	0.5	-
W	0.04	0.0005	-
R	3.0	3.0	-
σ_m(ksi) ($^{\text{tension}}_{\text{cutoff}}$)	0.010	1.5	0.667

Calculational Grids and Time Steps

Based upon previous experience with problems of this type and due to the desire to keep the calculational cost down, it was decided that a coarse mesh would be adequate for these problems. The meshes for problems P1, P2 and P3 are illustrated in Figs. 1, 2 and 4, respectively. The time increment for P1 and P2 was 1 millisecond and for P3 was 0.4 milliseconds. Thus, 250 time steps were used in P3 and only 100 time steps in P1 and P2. The P3 mesh had 1,089 elements and was run without using external storage. The P2 mesh had 4,840 elements and thus required external storage, since fewer than 2,000 elements fit in main memory at one time. Variable mesh generation was tested in P3 whereas P1

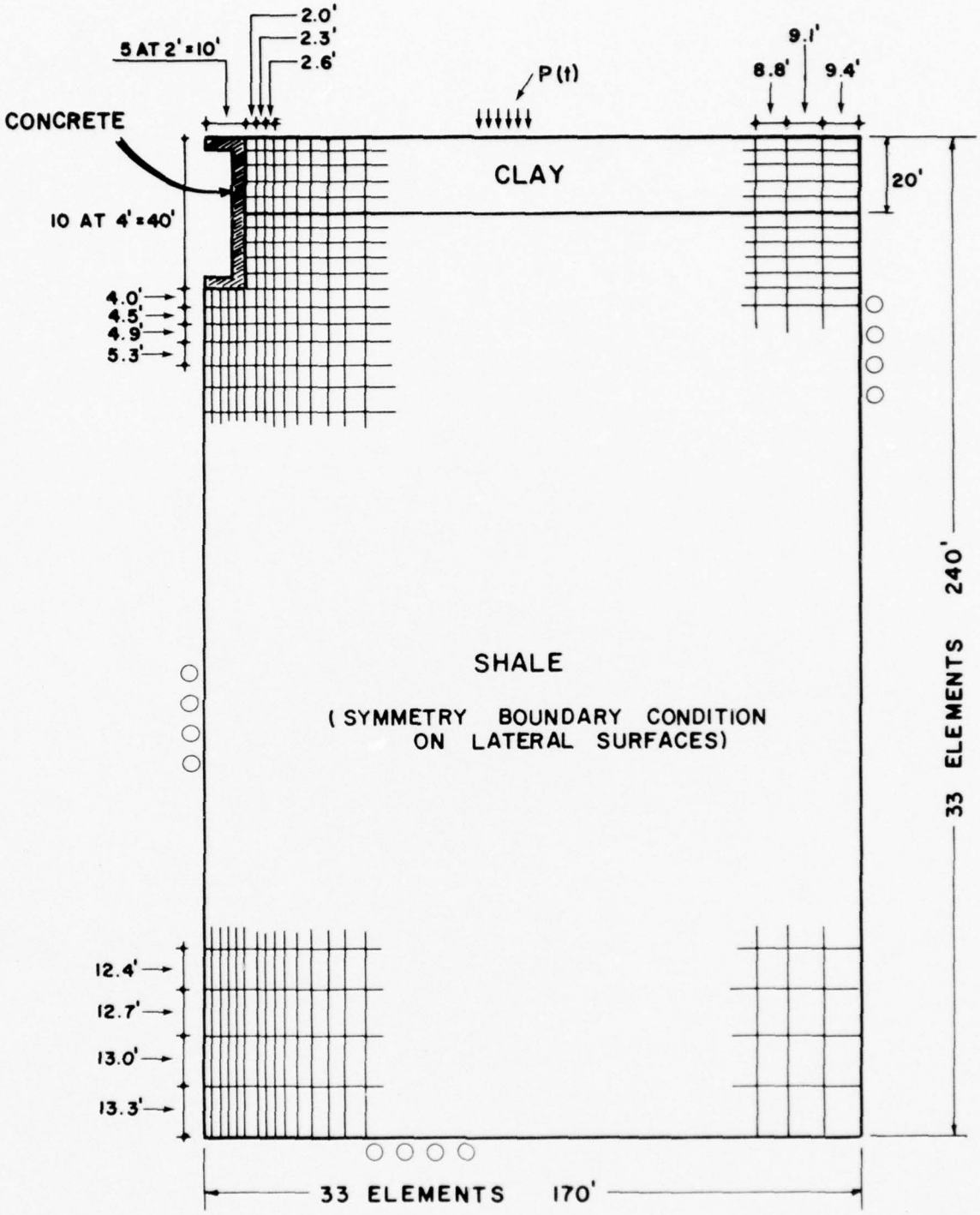

FIG. 4 PROBLEM P3 - FINITE ELEMENT MESH

and P2 used only two mesh sizes. Thus, a variety of important features of the code were exercised. The cost of running problems P1, P2 and P3 on the CDC 6600 was less than $2.00, $150.00 and $75.00, respectively.

IV NUMERICAL RESULTS

Problem P1

The vertical velocity and displacement histories for problem P1 from TRANAL at a depth of 2.9 ft are shown in Fig. 5. Also shown in this figure are the corresponding results from the LAYER code. The results from TRANAL and LAYER compare quite well when the coarseness of the mesh and other code details are considered. Some of the differences can be ascribed to

- time phasing details in applied surface loading
- different modeling of tensile behavior
- different approximation techniques (finite element and fintie difference)

The maximum velocity of about 360 in/sec is quite close to the theoretical value expected from simple, one dimensional shock considerations. This value can be obtained by using the shock condition

$$\Delta v = \frac{\Delta p}{\sqrt{\rho M}}$$

where Δp is the jump in pressure at the shock front, Δv is the jump in particle velocity, ρ is the material density and M is the secant modulus (Rayleigh line slope) corresponding to the shock loading of the material. From the stress-strain curve in Fig. 1, the 600 psi level corresponds to a strain of about 0.04; thus M = 15 ksi. The clay density, in consistent units, is ρ = .18. Since Δp = .6 ksi, the value of Δv is about 360 in/sec.

Although not shown in this report, time histories at

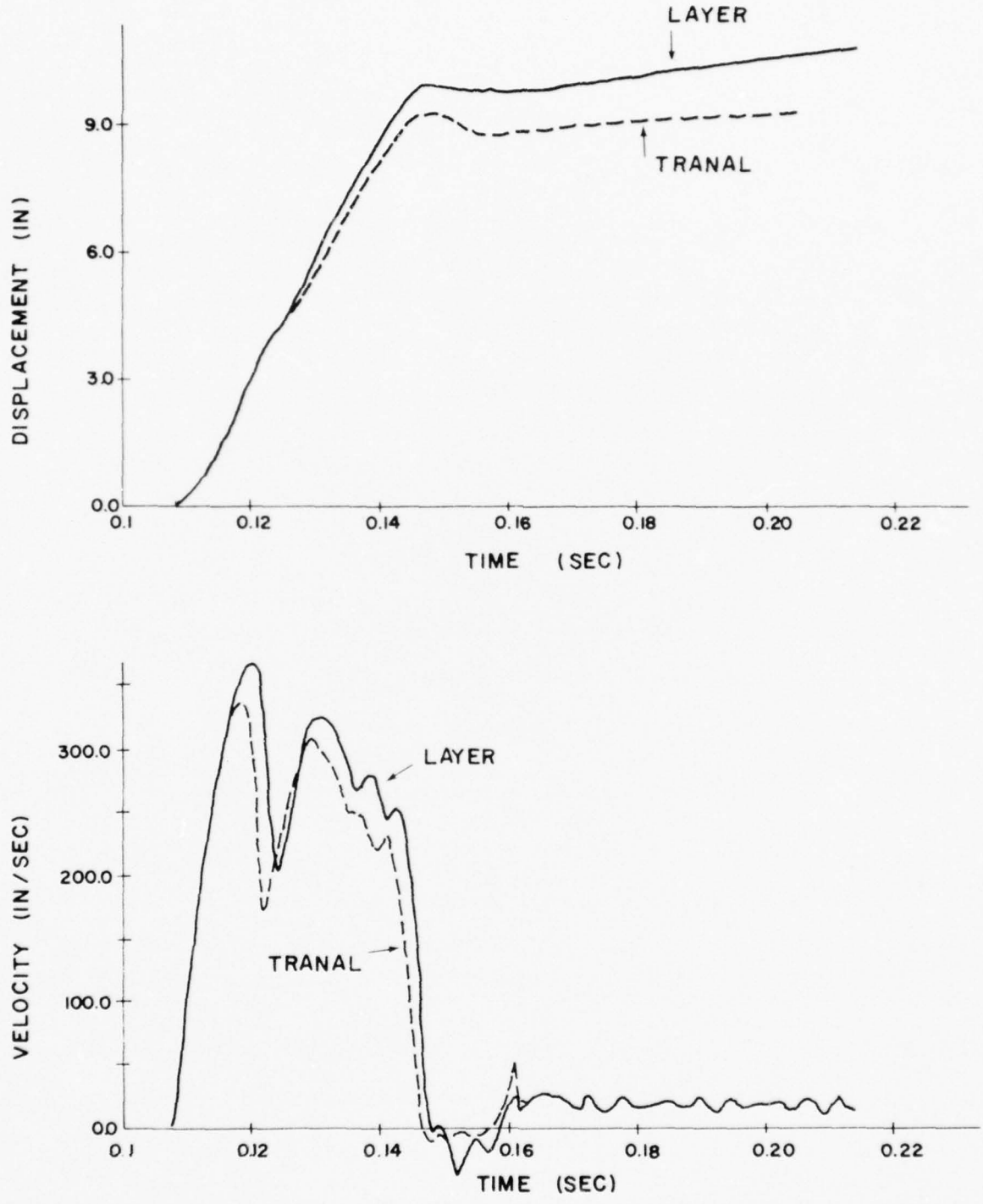

FIG. 5 PROBLEM PI - VERTICAL RESPONSE AT DEPTH = 2.9 FT.

other depths compare equally well when TRANAL and LAYER results are examined. Additional comparisons are presented in the following discussion of the two dimensional problem P2.

Problem P2

Velocity and displacement histories in both the radial and vertical directions are shown in Figs. 6-10. Corresponding time histories from the LAYER code are also shown in these figures. Once again the agreement is seen to be quite good when the factors mentioned for problem P1 are considered.

The largest percentage difference seems to appear in Fig. 7, where the maximum radial velocity at the near surface point is more than 100 in/sec in the TRANAL calculation and only 70 in/sec in the LAYER calculation. The displacements are, however, better. This is normally the case in finite difference and finite element wave propagation calculations of this type. Generally speaking, maximum velocities are less reliable than displacements since the nature of wave motion is that displacements are continuous whereas velocities may be discontinuous. This is particularly the case near boundaries and interfaces. In addition, peak values of velocity (vertical and radial) are sensitive to the introduction of viscosity. Neither the LAYER or the TRANAL calculation used artificial viscosity. Furthermore, modification of the rise time of the applied surface loading can affect the peak velocity. In both calculations, the rise time was not modified so that the effective rise time of the load was controlled by the speed of the load and the mesh size. Slight differences in phasing of the applied

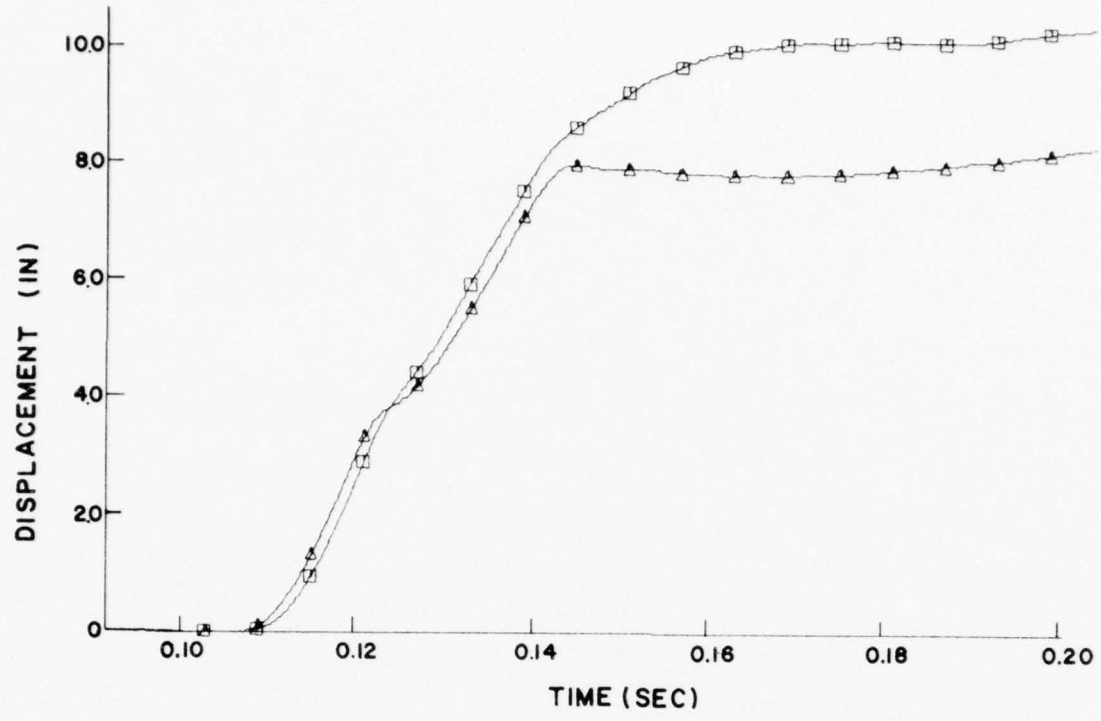

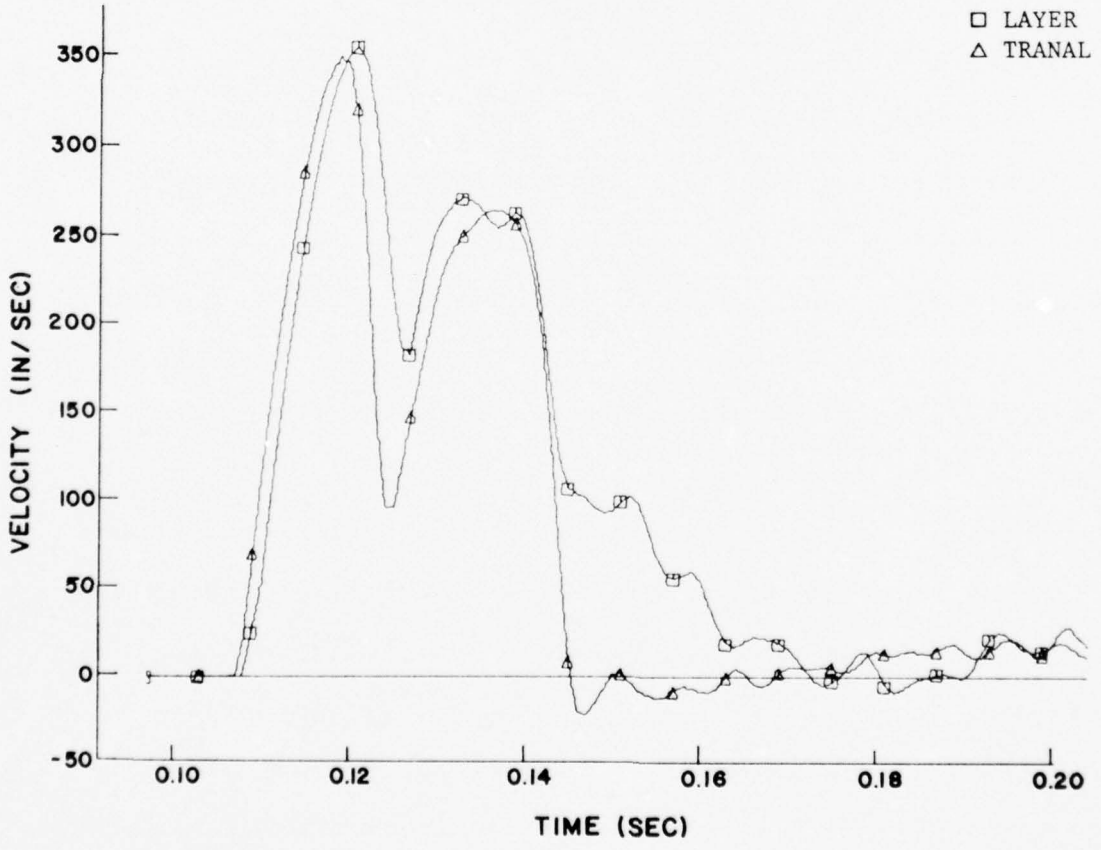

FIG. 6 PROBLEM P2 - VERTICAL RESPONSE AT RANGE = 1840 FT. DEPTH = 2.9 FT

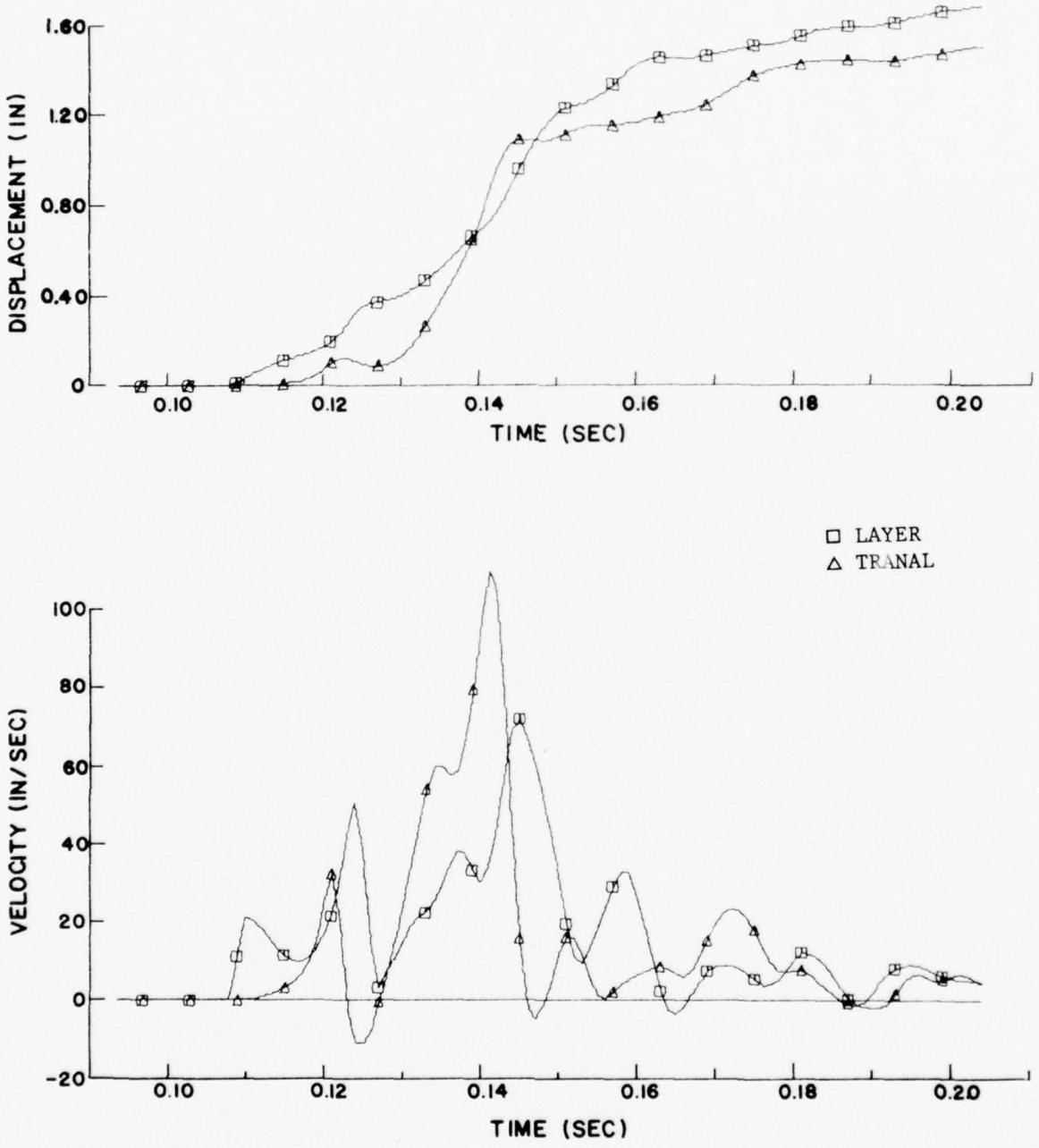

FIG. 7 PROBLEM P2 RADIAL RESPONSE AT RANGE = 1840 FT. DEPTH = 2.9 FT.

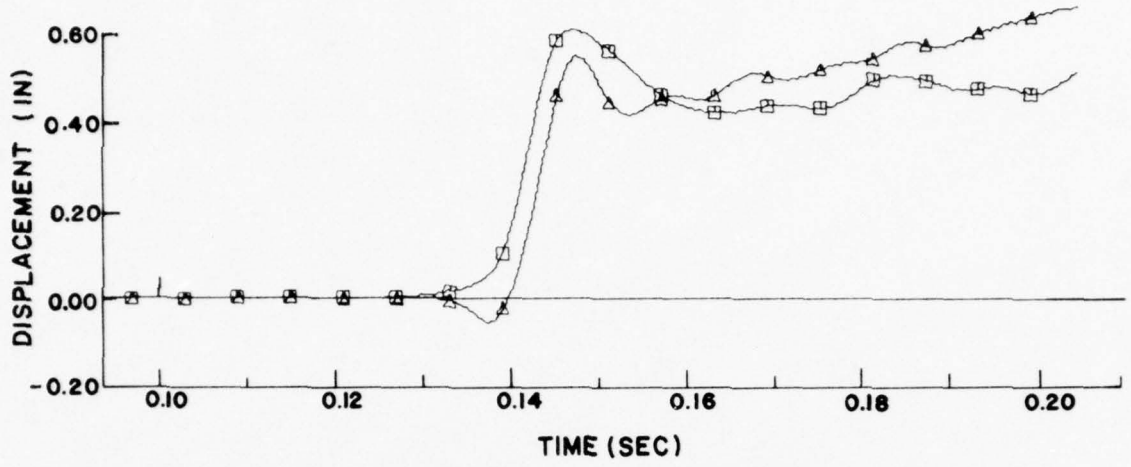

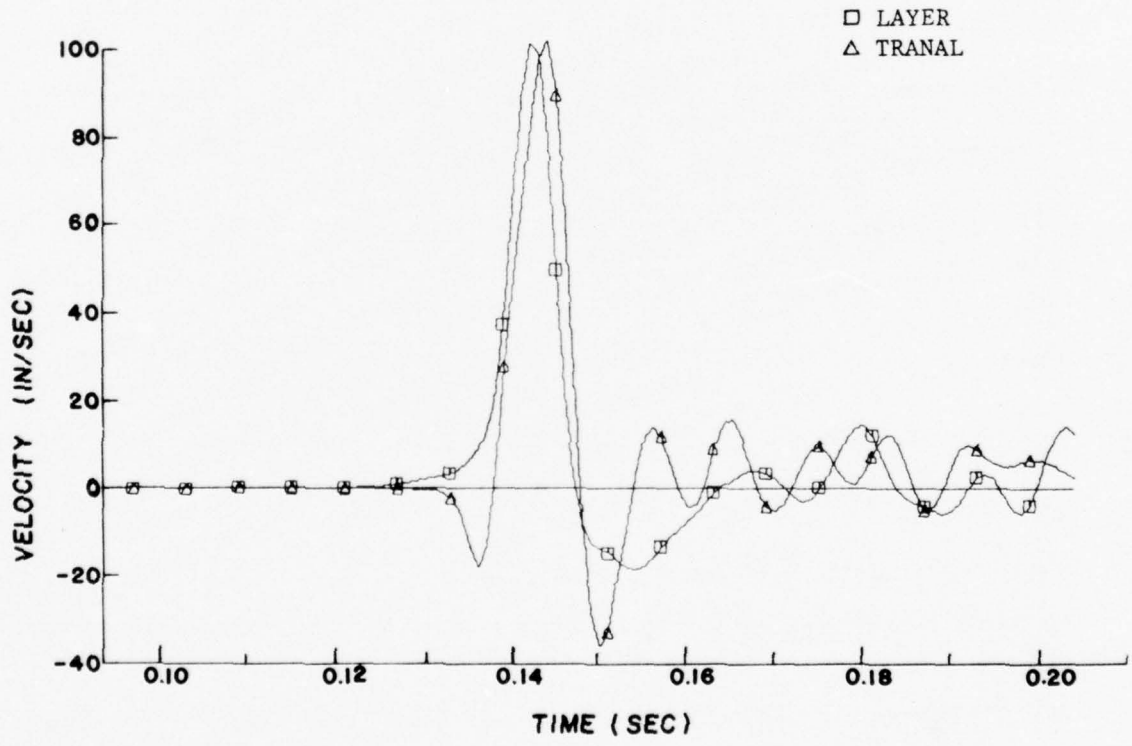

FIG. 8 PROBLEM P2 - RADIAL RESPONSE AT RANGE = 1840 FT. DEPTH = 20 FT.

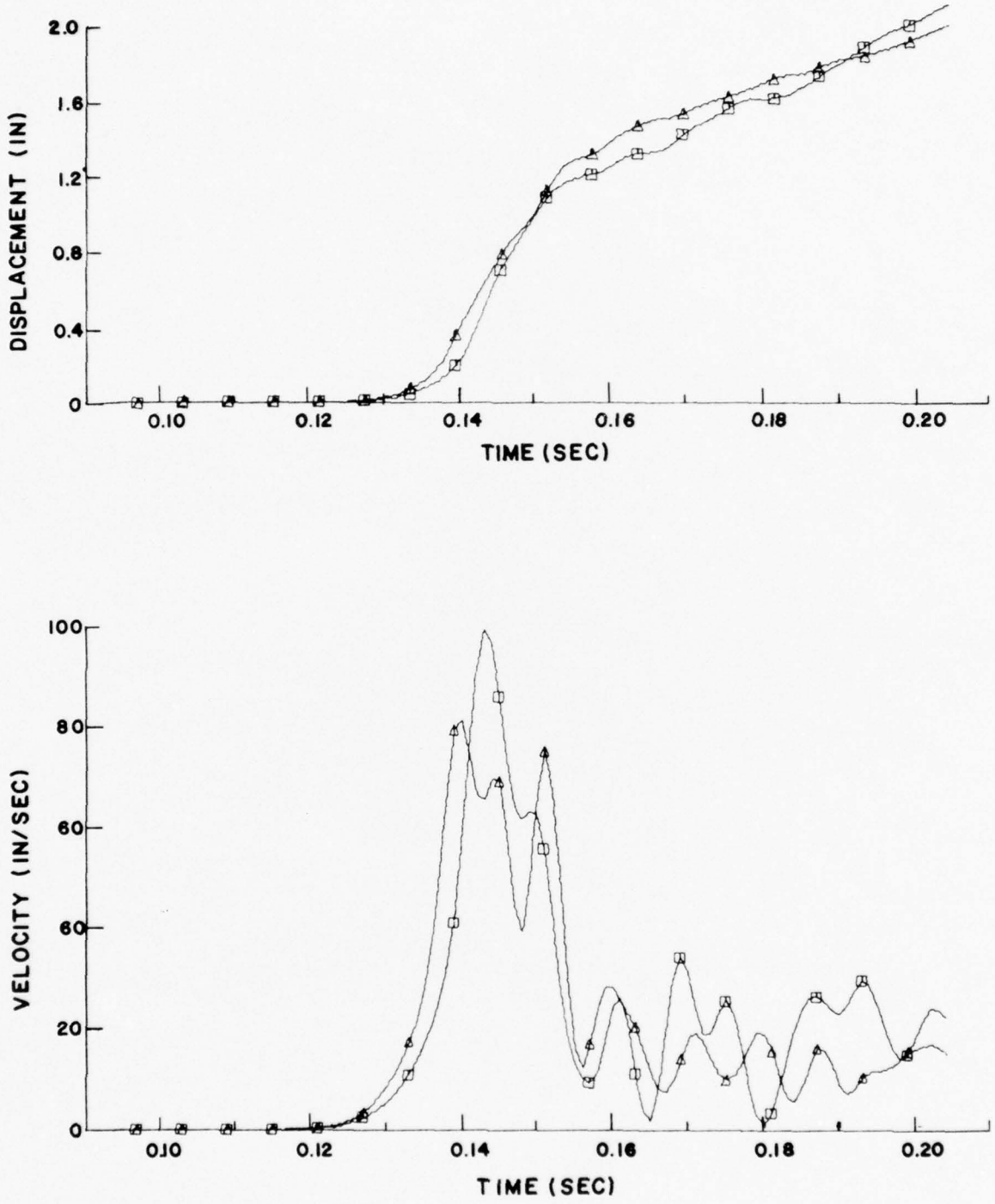

FIG. 9 PROBLEM P2 - VERTICAL RESPONSE AT RANGE = 1840 FT. DEPTH = 30 FT.

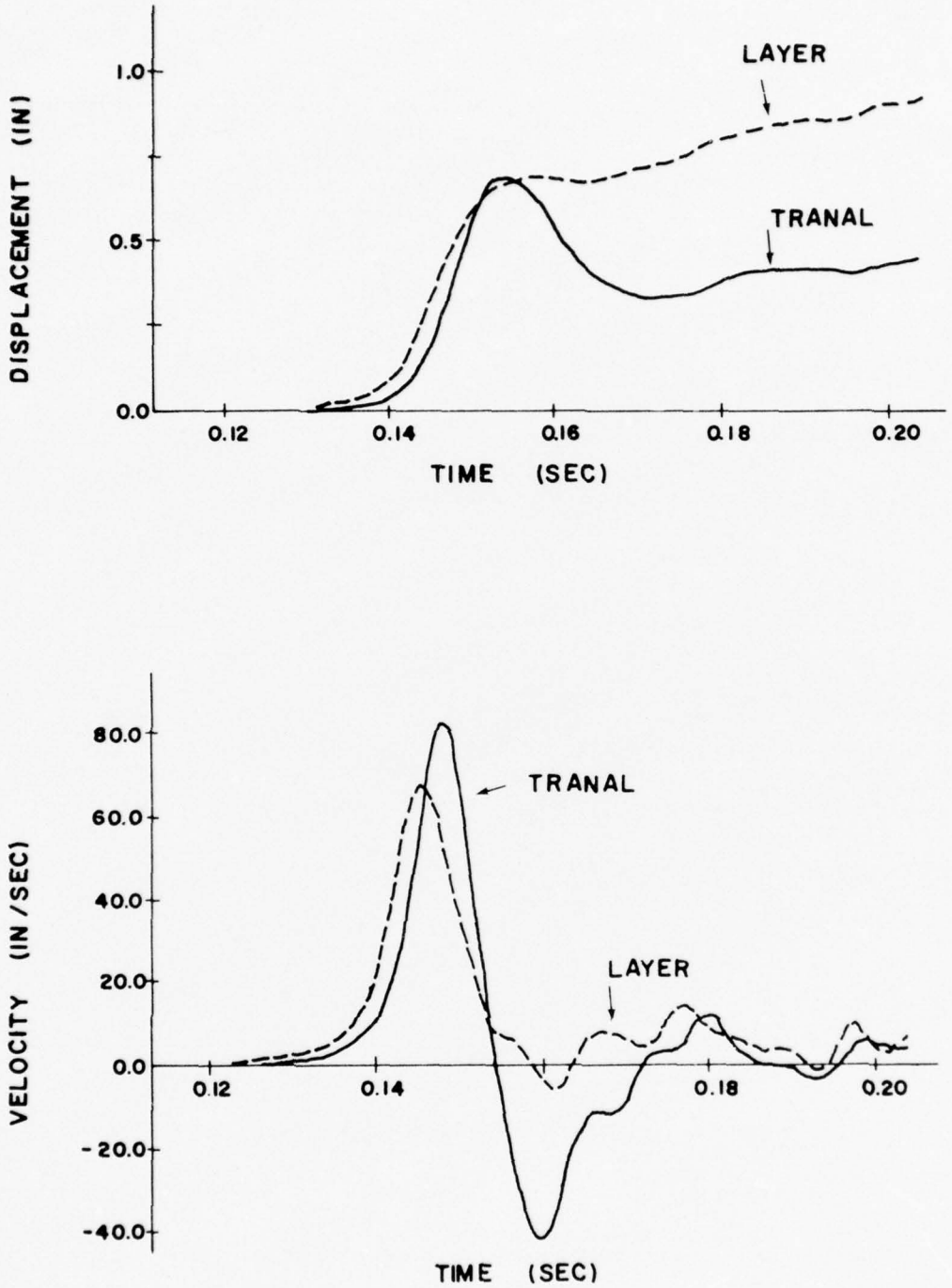

FIG. 10 PROBLEM P2 RADIAL RESPONSE AT RANGE = 1840 FT. DEPTH = 40 FT.

load can then lead to noticeable changes in a potentially discontinuous quantity such as velocity (or stress). Displacements are generally better behaved as observed.

In this problem, the airblast shock front is traveling at about 7 ft/msec at the range of interest. The loading wave speed in the clay is less than 1 ft/msec which leads to a highly supersonic loading front in the clay. Thus radial motions are generally small (compared to the vertical) at the loading front and are affected substantially (percentage wise) by differences in phasing. After the loading front has reflected from the clay-shale interface, larger radial motions appear. However, by this time the coarse mesh coupled with the discontinuous behavior of the velocities has resulted in what appears to be a substantial error in the radial velocity. In fact, the difference noted in Fig. 7 of 35 in/sec between LAYER and TRANAL is only 10 per cent of the maximum velocity felt at that point in the vertical direction. In short, radial velocities will always appear unreliable in finite element and finite difference calculations of this type if they are viewed on an absolute scale. It is necessary instead to consider both components of the velocity in order to judge the results. With this point of view in mind, approximate values of maximum response for several depths are presented in Table II.

TABLE II. MAXIMUM RESPONSE WITH DEPTH
(during first 100 milliseconds)

Depth (Ft)	Displacements (in)		Velocities (in/sec)	
	Vertical	Radial	Vertical	Radial
0	12	1.2	400	100
10	7	1.5	300	100
20	2	.6	100	100
30	2	.6	80	80
40	2	.6	80	80

The results in Table II are given with only one or two significant figures because of the above reasons. A few observations are in order however.

A vertical surface displacement of about 12 inches is quite reasonable for the highly hysteretic clay used. Maximum compaction at 600 psi is about 4 per cent. Since the clay layer is 20 ft. deep, the maximum displacement should be about 0.4 x 20 = .8 ft, or about 10 inches relative to the interface as observed.

The shale has very little hysteresis (see Fig. 1) and thus there should be little change with depth below 20 ft, as shown in Table II.

The shale has a wave speed of about 4.8 ft/msec. At this rate the loading front in the shale should be at about 45 degrees to the interface. Since the maximum velocity in the shale occurs at the loading front, the jump in vertical and radial velocities should be nearly equal below 20 ft, as shown in the table.

Problem P3

Selected motion and stress histories for problem P3 from TRANAL are shown in Figs. 11-20. It should be noted that, away from the structure, the motions for problem P3 are practically identical to those of problem P1, as they should be. Such comparisons have not been reproduced here since they would merely duplicate results in Figs. 5-10.

It should also be noted that certain conclusions are drawn here which are obtained by studying integrated quantities such as displacements and impulses. As discussed for problem P2, integrated quantities are more reliable due to the nature of wave propagation calculations of this type than are quantities such as maximum velocity or maximum stress. This is particularly true for a coarse grid calculation such as the one used here.

By looking at a point quite near the structure, it is possible to observe the similarity of the free-field motions (problems P1 and P2) to the results from problem P3. For example, Fig.12 shows a point two feet away from the top corner on the clay surface which should be compared with Fig. 5. In both cases, the displacement rises quickly but smoothly to a value of about 9 inches in less than 40 milliseconds and then rises slowly during the next 60 milliseconds to a maximum of about 10 inches or so. In essence then, the vertical motion of the clay surface is not significantly modified by the presence of the structure.

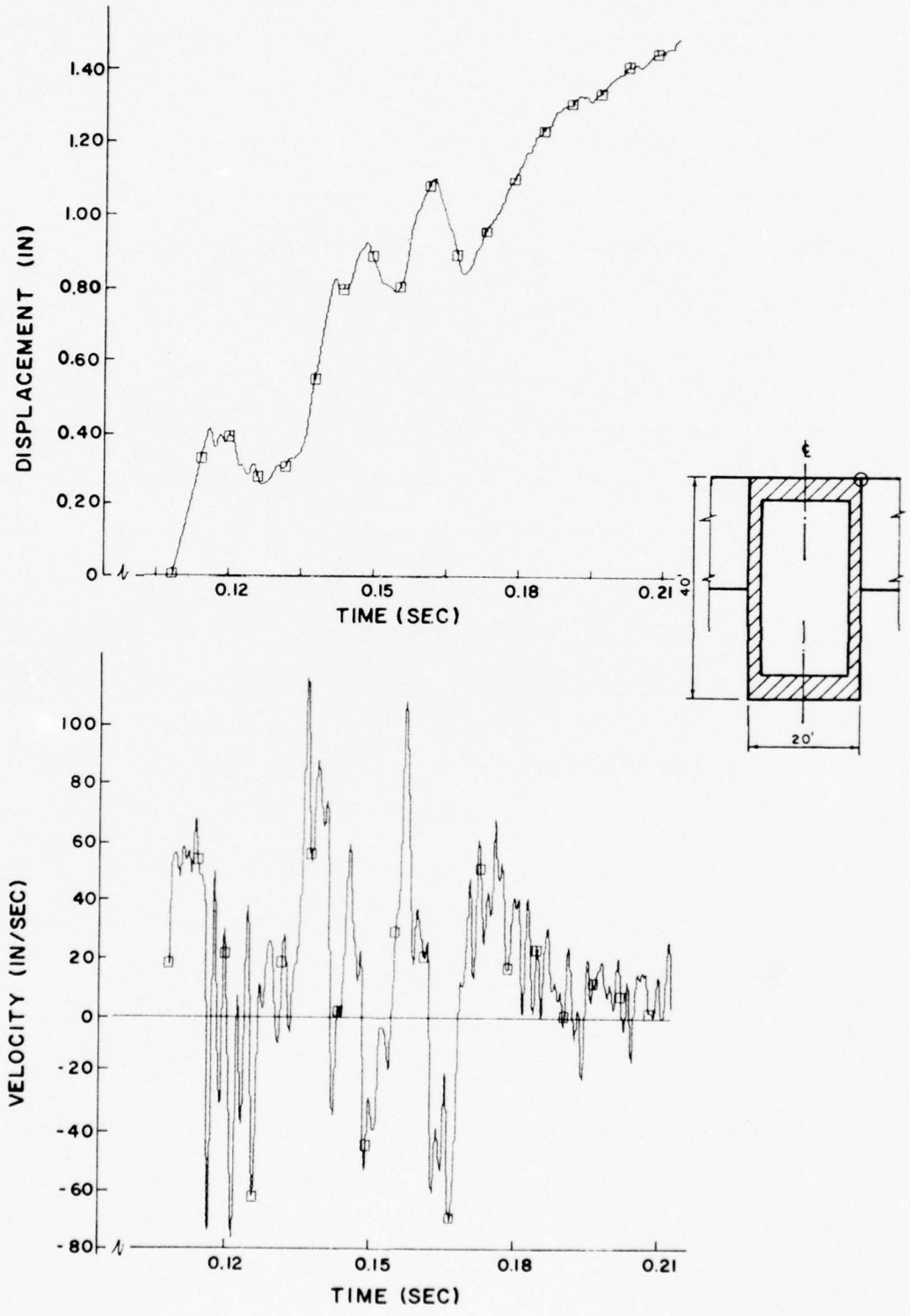

FIG. 11 PROBLEM P3 - VERTICAL RESPONSE, THE TOP CORNER OF STRUCTURE

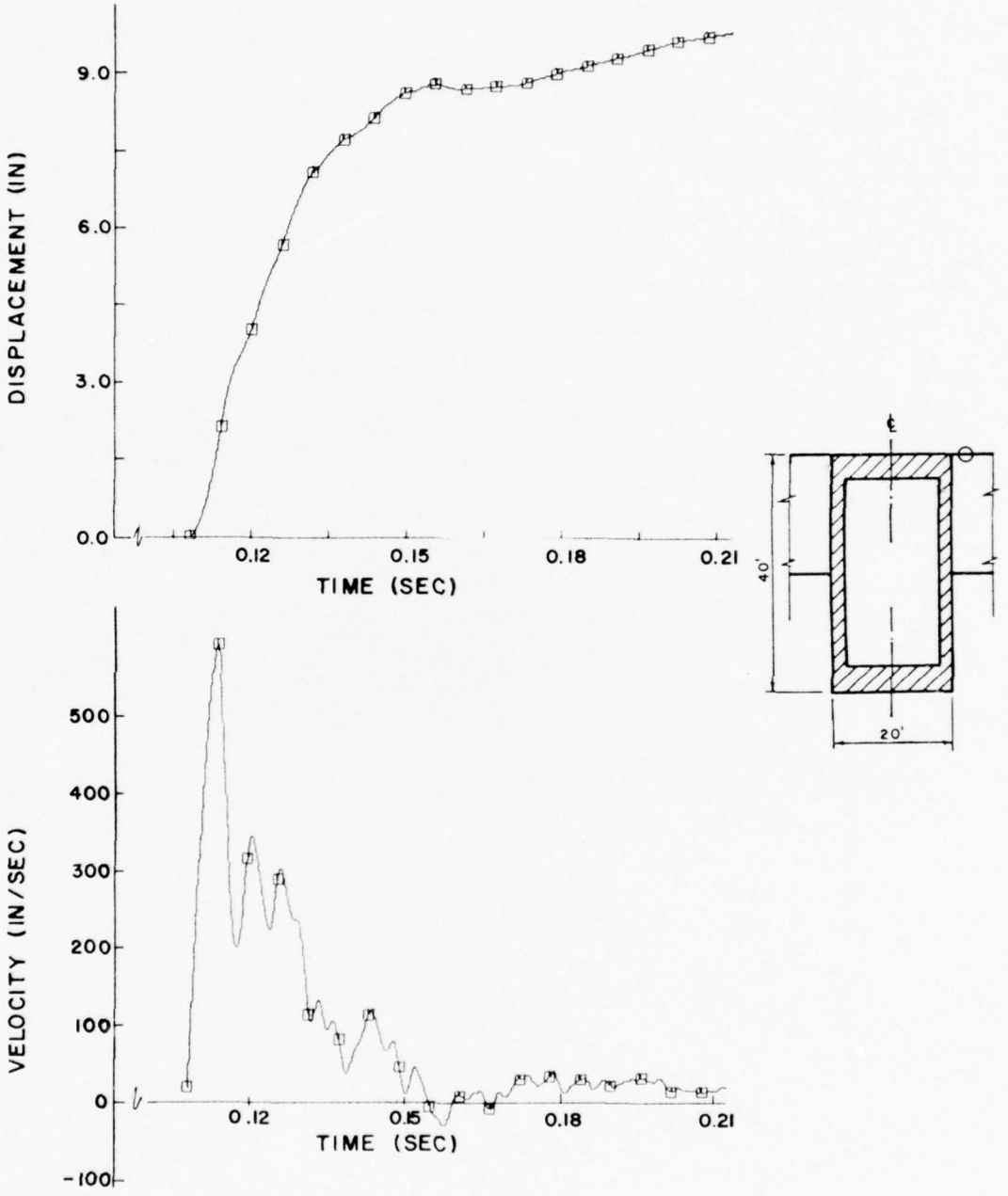

FIG. 12 PROBLEM P3 - VERTICAL RESPONSE 2 FT AWAY FROM TOP CORNER OF STRUCTURE

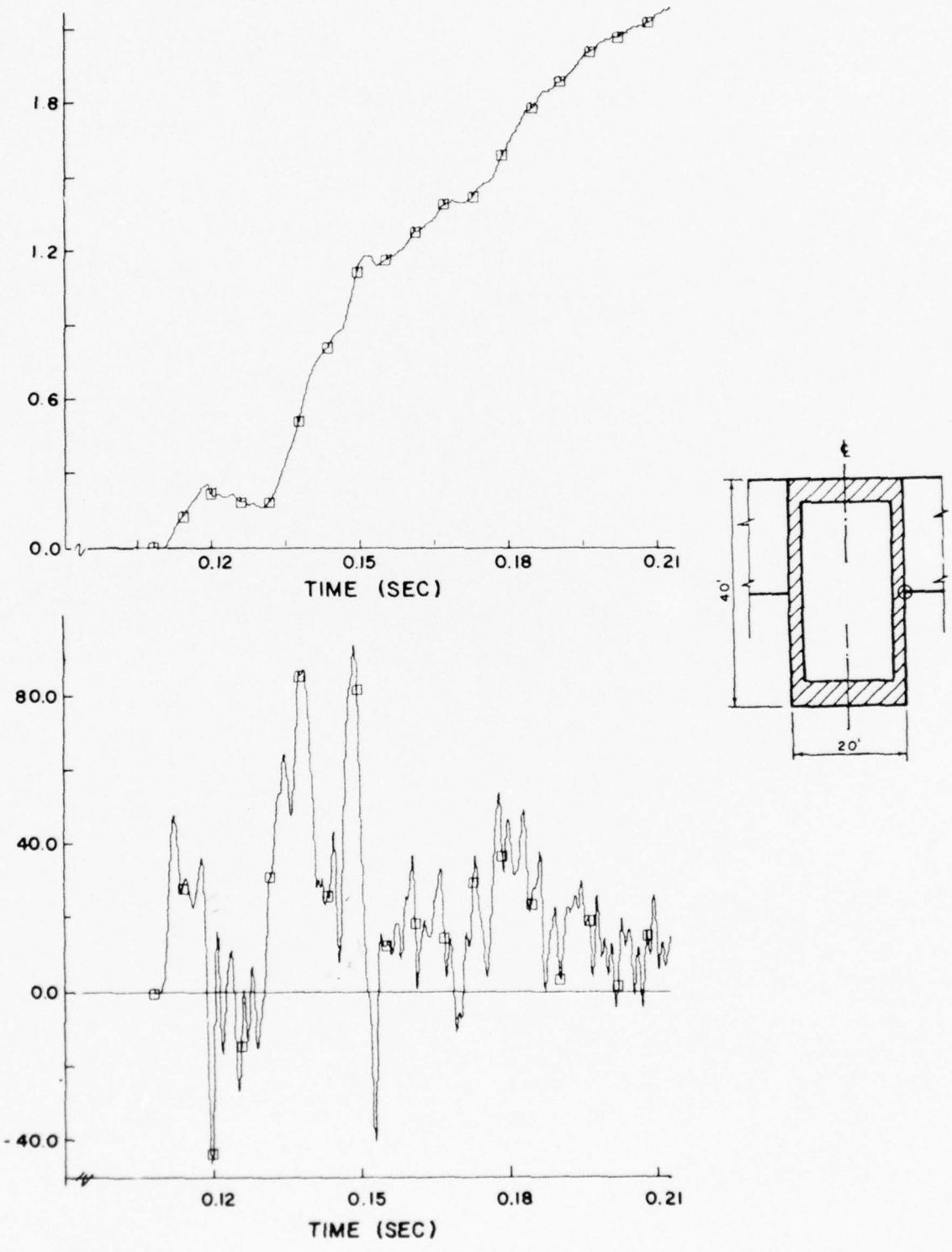

FIG. 13 PROBLEM P3 - VERTICAL RESPONSE AT THE CLAY - SHALE - CONCRETE INTERSECTION

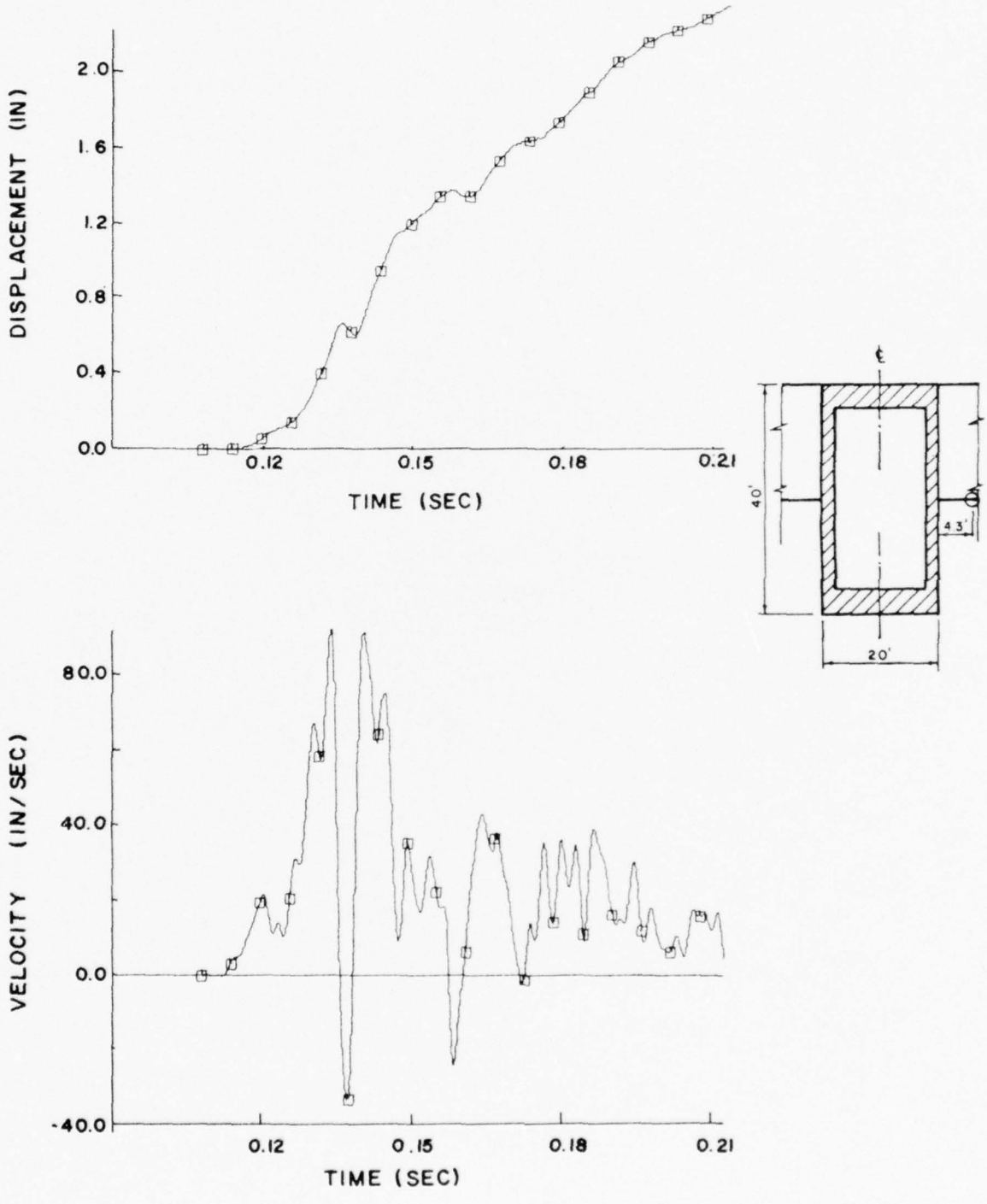

FIG. 14 PROBLEM P3 - VERTICAL RESPONSE AT THE CLAY-SHALE INTERFACE, 4.3 FT AWAY

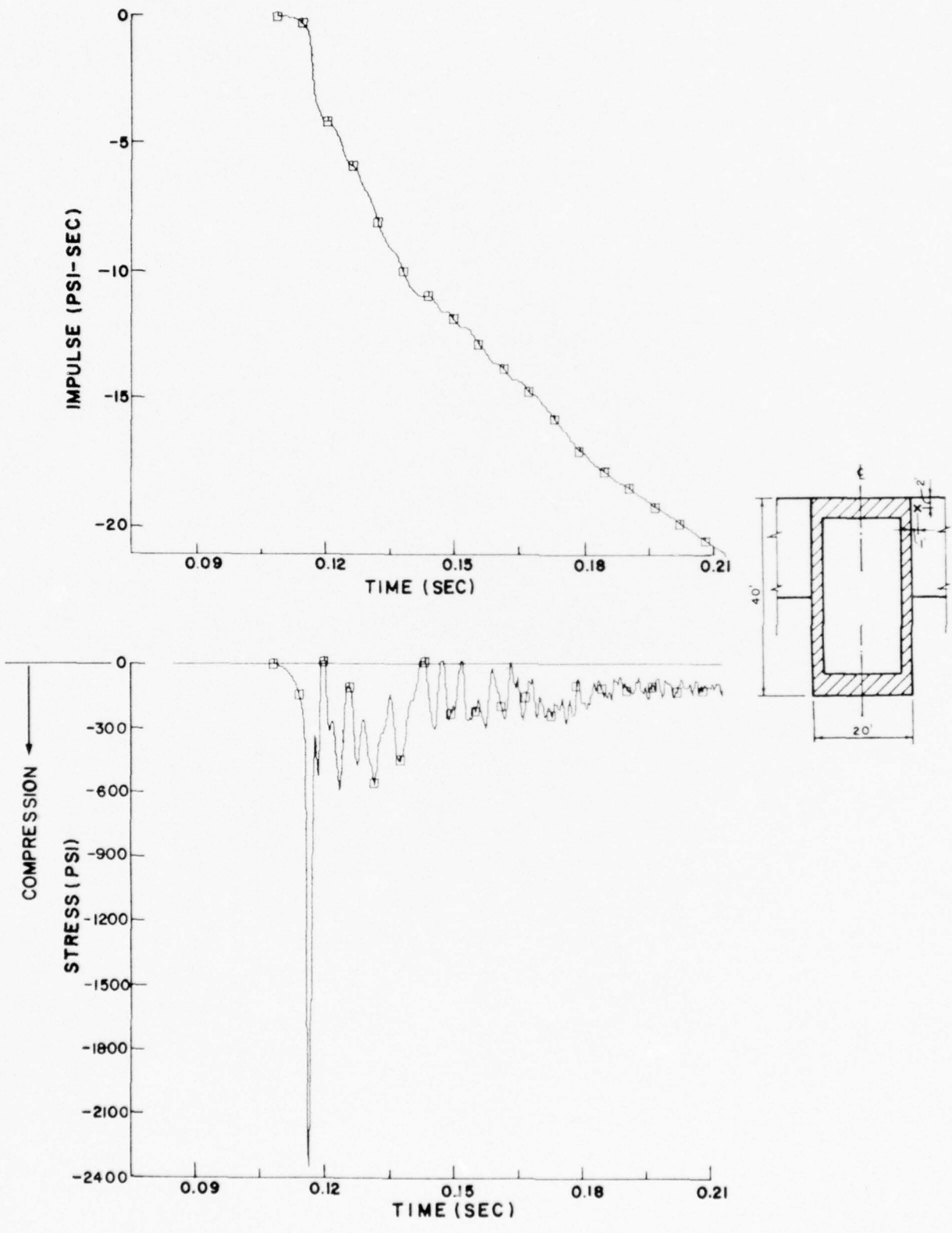

FIG. 15 PROBLEM P3 - VERTICAL STRESS AND IMPULSE NEAR TOP CORNER OF STRUCTURE, 1 FT AWAY

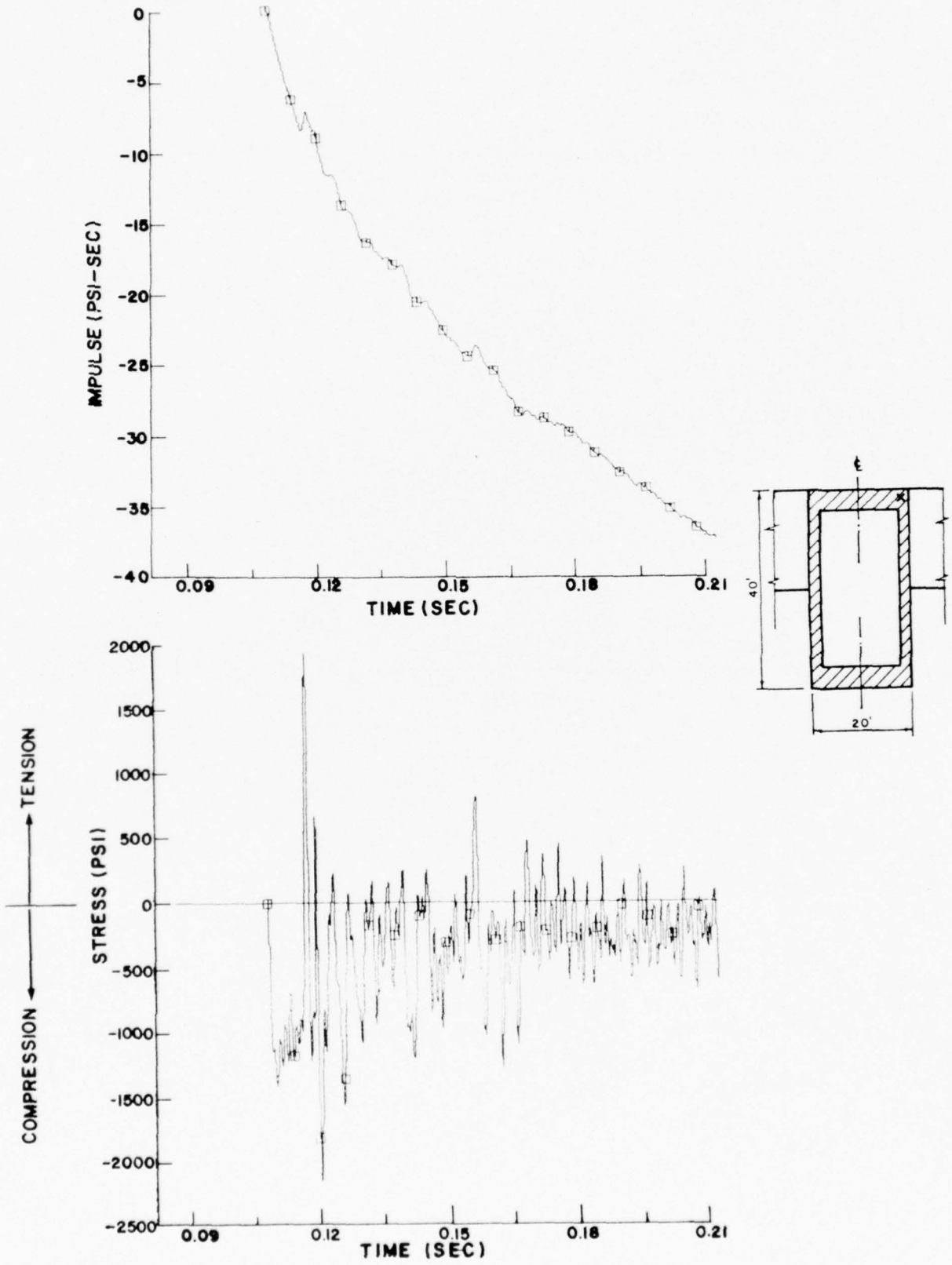

FIG. 16 PROBLEM P3 - VERTICAL STRESS AND IMPULSE IN TOP CORNER OF STRUCTURE

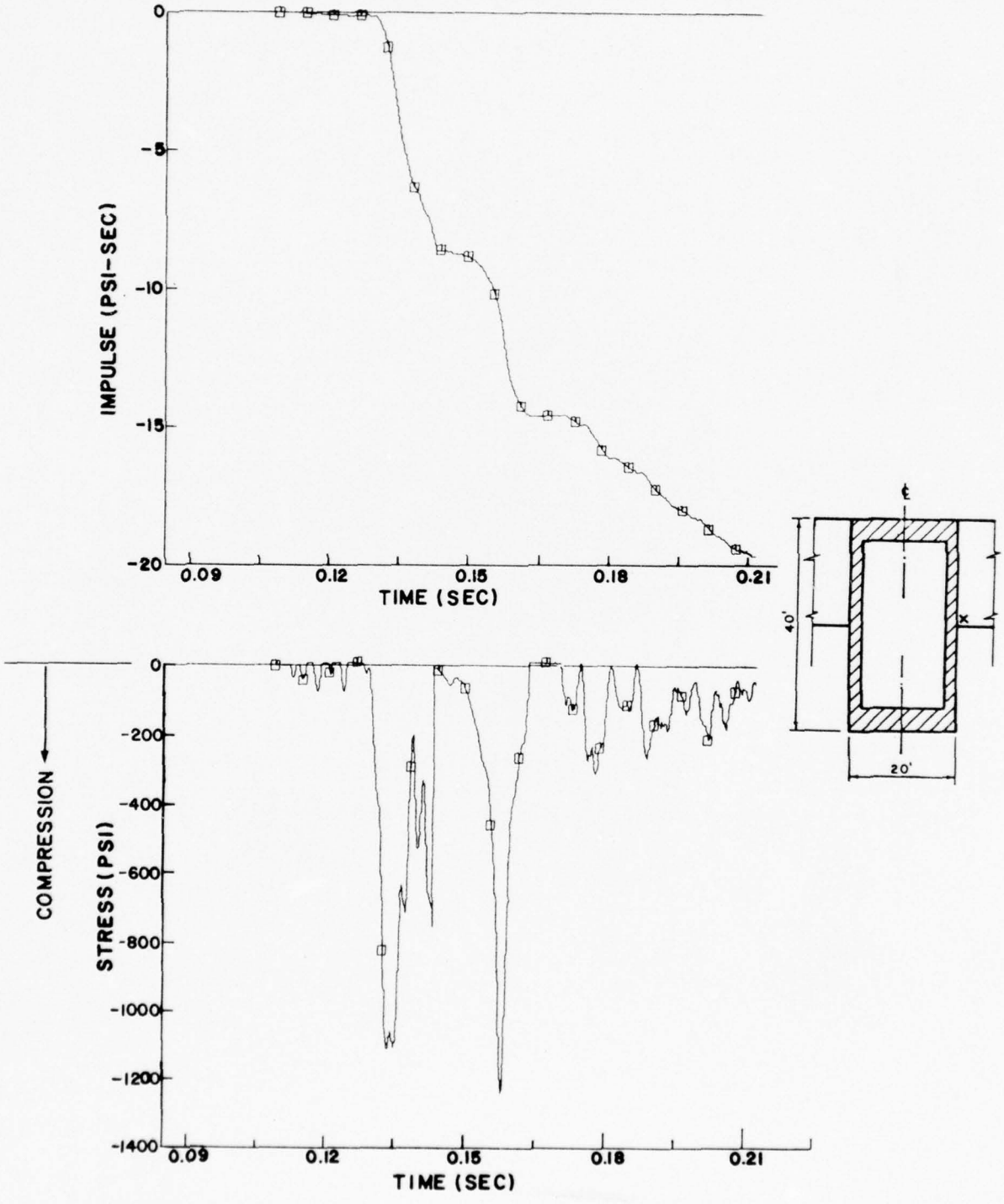

FIG. 17 PROBLEM P3 – VERTICAL STRESS AND IMPULSE 2 FT. ABOVE CLAY SHALE INTERFACE, 1 FT AWAY

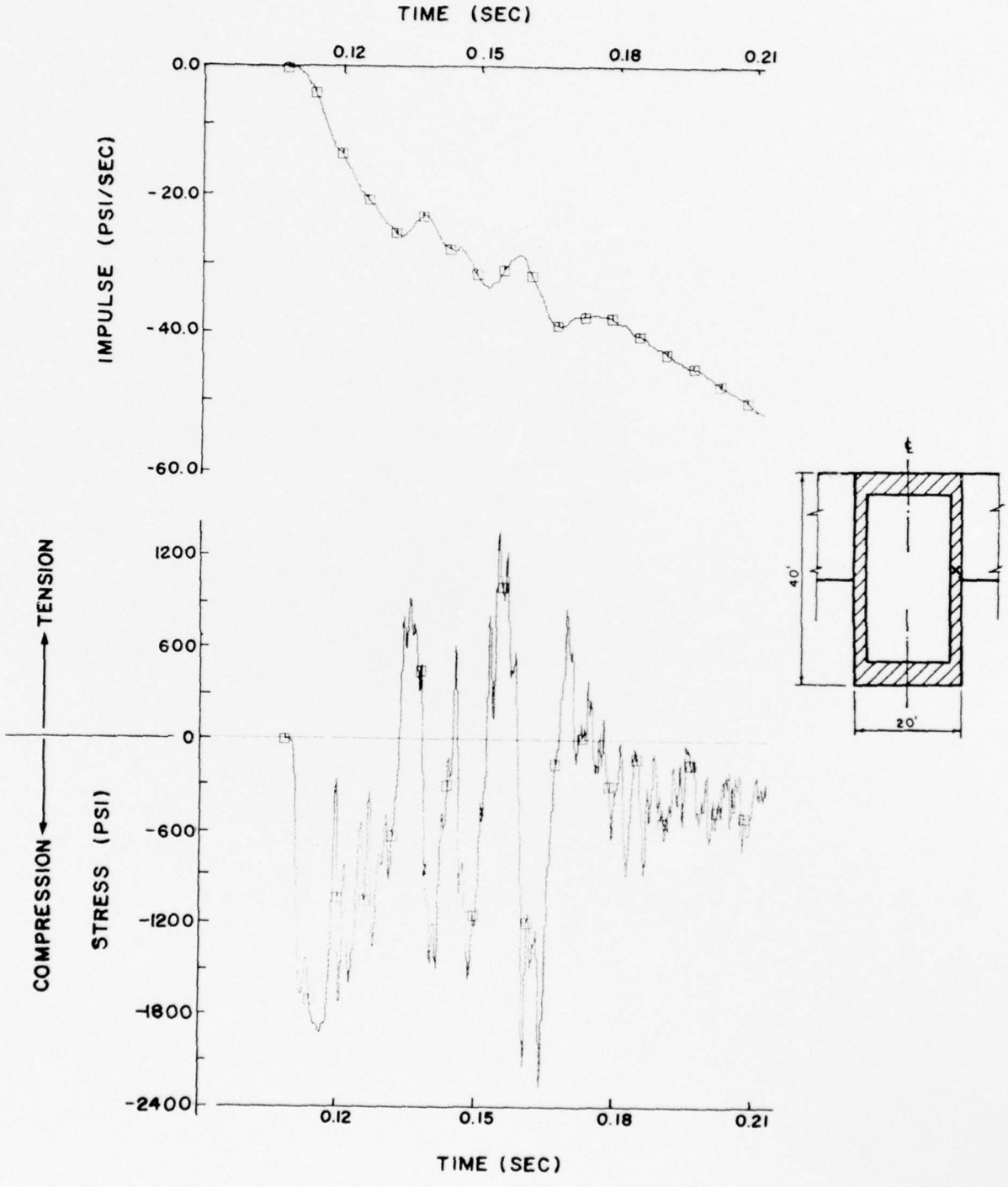

FIG. 18 PROBLEM P3 - VERTICAL STRESS AND IMPULSE IN SIDE WALL OF STRUCTURE

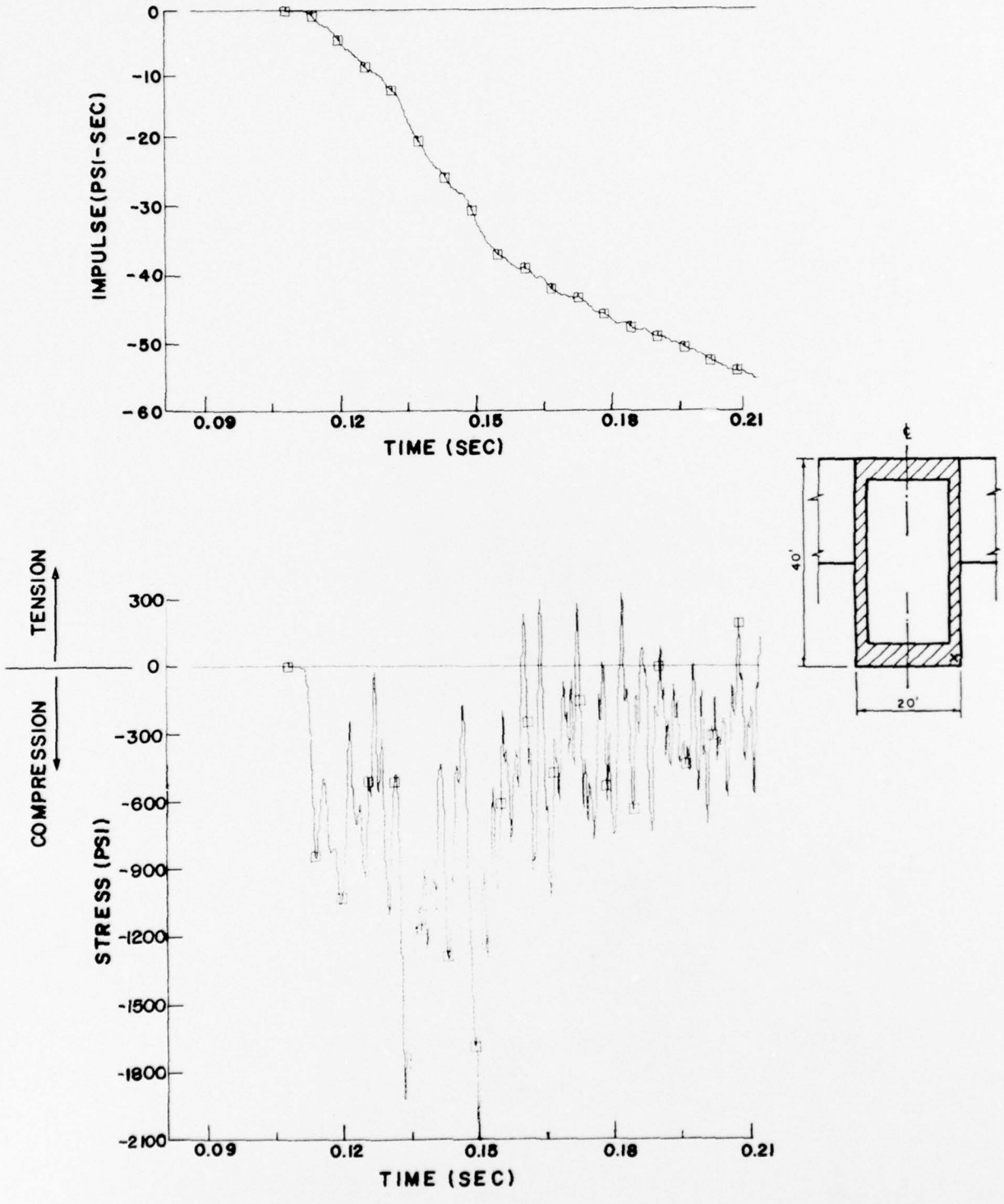

FIG.19 PROBLEM P3 - VERTICAL STRESS AND IMPULSE IN BOTTOM CORNER OF STRUCTURE

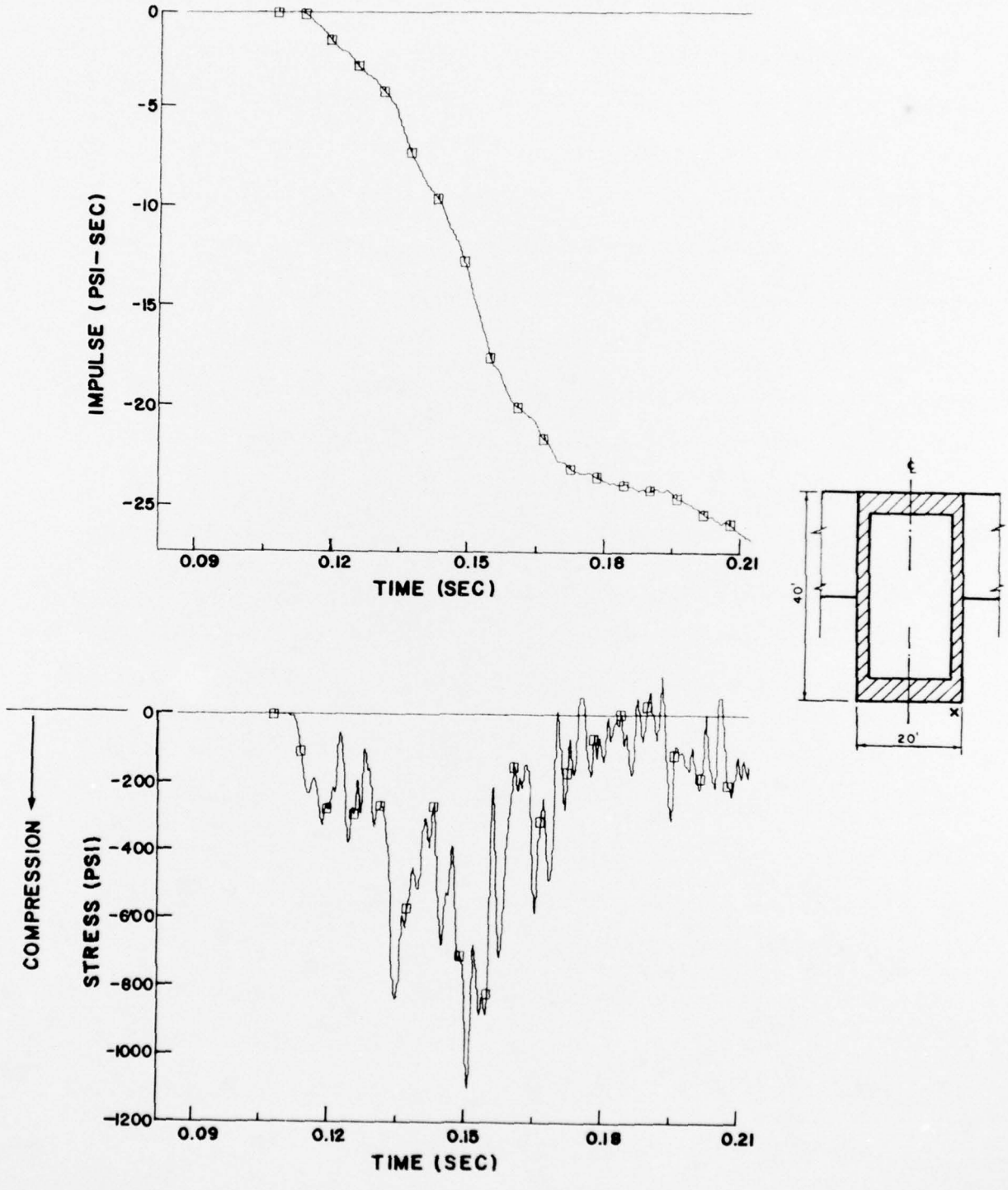

FIG. 20 PROBLEM P3 VERTICAL STRESS AND IMPULSE 2 FT BELOW BOTTOM CORNER OF STRUCTURE

On the other hand, the motion of the structure itself is quite different from the surrounding clay at the surface. As can be seen in Fig. 11, the top corner of the structure deflects rapidly about 0.4 inches, reverses slightly about 0.1 inches, further deflects quickly to about 0.9 inches, oscillates twice at roughly this level with an amplitude of about 0.1 inches and then deflects to a maximum displacement of about 1.6 inches. The oscillatory motion has a period of about 16 milliseconds. Since the dilatational wave speed of the concrete is about 10 ft/msec and its height is 40 ft., this period is just the time required for a wave to travel four times the height of the concrete. Four times is the correct number needed for a wave front to reflect (i) from the bottom, (ii) then the top, (iii) again the bottom and finally (iv) the top so that the velocities and stresses are both back in phase with the original wave front.

Again, by looking at a point about 4 ft. from the side wall of the structure, it is a simple matter to observe the similarity of the free-field motion and the results of problem P3. In particular, Fig. 14 should be compared with Fig. 9. In both cases the displacement rises to a value of about 1.4 inches in 30 milliseconds and then rises more slowly during the next 60 milliseconds to a peak of about 2.2 inches. Maximum velocities of about 100 in/sec occur in each case. Naturally, high frequency motions are affected as can be seen by comparing the velocity waveforms. However, judging from the displacements, the free-field is not significantly altered by the structure.

The maximum vertical impulse imparted to the surface during the first 100 milliseconds is about 22 psi-secs (calculated from the Brode simple fit, Ref. [5]). Figure 15 shows that the maximum impulse in the clay at a point near the top corner of the structure is about 21 psi-secs. Figure 17 shows a similar value of 20 psi-secs at a depth of 18 ft in the clay at a point next to the concrete wall. This indicates that the impulse imparted to the surface is conducted vertically through the clay to the interface without significant modification. On the other hand, the concrete structure has maximum impulse values in the wall of 52 and 54 psi-secs, as shown in Figs. 18 and 20. This is due to the fact that the load applied over the entire surface of the structure must be conducted down the relatively thin walls since the cylinder is hollow. In fact, the ratio of the wall impulse, I_w, to the surface impulse, I_s, should have the same value as the ratio of the top surface area of the structure to the wall area through which the vertical stress is conducted; that is,

$$\frac{I_w}{I_s} \approx \frac{A_s}{A_w} = \frac{10^2}{10^2-8^2} = 2.77$$

Since I_s is about 22 psi-sec, the value of I_w should be about 61 psi-secs. The fact that the peak is somewhat less in Figs. 18 and 20 probably reflects the fact that some impulse is transmitted to the surrounding soil (although not much).

Maximum stress values, while somewhat unreliable in this calculation, were always less than 2,400 psi in the concrete walls and, except for short durations (a few milliseconds),

maximum stresses in the side walls were less than 2,000 psi which is much less than the assumed compressive strength (6,000 psi) of the concrete. This indicates that the walls of the structure will not fail in compression from a load of the type used in problem P3.

The largest observed stress anywhere in the structure was less than 6,000 psi and occurred in the middle of the top for about one millisecond. The calculations for the top are not particularly reliable though since only one element was used through the roof and a great deal of bending and shear behavior was evident. Additional study would be required to resolve the question of whether or not the top could fail under the assumed loading. Tensile failure in the Structure, assumed to be 667 psi in mean pressure, was observed occassionally but only for short durations and thus did not appear to be important in this problem.

Thus, the picture that emerges from problem P3 when problems P1 and P2 are considered is that (i) the structure and the surrounding soil interact very little and (ii) the side walls of the structure can survive the type of loading prescribed for problem P3. Only the survival of the top of the structure is in doubt and this question can be studied more economically by other methods. If a rapidly expanding load is prescribed, as in problem P2, then additional modes of behavior (two and three dimensional effects) can lead to additional interaction phenomena.

However, it appears highly unlikely that the walls of this structure will fail from a loading of this type during the first 100 milliseconds (which is probably the most critical period).

V SUMMARY AND CONCLUDING REMARKS

Vulnerability problems of interest to SAMSO require the simulation of soil-structure interaction effects due to nearby explosions. The SAMSO-TRW test problems have been used to check out various features of the TRANAL code and many of the capabilities required for such studies have been demonstrated.

For two of the test problems, TRANAL and LAYER results were compared and the differences can be understood in terms of code details such as surface pressure phasing and approximation techniques (finite element and finite difference).

The third problem, which involves an embedded hollow cylinder, is studied and it is concluded that, for the prescribed loading, (i) the structure and surrounding soil interact very little and (ii) the side walls of the structure will survive. However, these conclusions are based on a simple two dimensional, axisymmetric problem. In order to understand the vulnerability problem more fully, it is necessary to examine a three dimensional problem with a more realistic structural model and site profile.

Studies of the HARD PAN I-3 event are now under way (under SAMSO contract) in order to study a full 3-D case. In order to reduce this problem to manageable proportions, the soil-island method, Ref. [7], is being used with soil-island boundary motions produced from the LAYER code.

REFERENCES

[1] Wright, J.P., "3-D Structure-Medium Interaction Calculations", presented at DNA Strategic Structures Review Meeting, Stanford Research Institute, Menlo Park, California, February 1975.

[2] Baylor, J.L. and Wright, J.P., "Three Dimensional Nonlinear Analysis", in Finite Element Analysis of Transient Nonlinear Structural Analysis, A.S.M.E., AMD-Vol 14, Winter Annual Meeting, Houston, Texas, pp. 179-191, December 1975.

[3] Baylor, J.L., Bieniek, M.P. and Wright, J.P., "TRANAL: A 3-D Finite Element Code for Transient Nonlinear Analysis", DNA 3501F, Weidlinger Associates, New York, New York, 1974.

[4] Sandler, I.S. and Rubin, D., "A Modular Subroutine for The Cap Model", forthcoming DNA report, Weidlinger Associates, New York, New York, January 1976.

[5] Brode, H.L., "Height of Burst Effects at High Over-pressures", DASA 2506, The Rand Corporation, Santa Monica, California, July 1970.

[6] DiMaggio, F.L. and Sandler, I.S., "Material Models for Granular Soils", Journal of Engineering Mechanics Division, ASCE, pp. 935-950, June 1971.

[7] Nelson, I., "Analysis of Soil Structure Interaction on Site Defense (SD) Type Semi-Buried Structures, Part 1", HND-TR-75-20-ED-CS, Weidlinger Associates, New York, New York, 1975.

DISTRIBUTION LIST

DEPARTMENT OF DEFENSE

Assistant Secretary of Defense
Intelligence
ATTN: ODASD IA

Assistant to the Secretary of Defense
Atomic Energy
ATTN: Honorable Donald R. Cotter

Director
Defense Advanced Research Projects Agency
ATTN: Tech. Lib.
ATTN: NMRO
ATTN: PMO
ATTN: STO

Director
Defense Civil Preparedness Agency
ATTN: Staff Dir., Research, George N. Sisson
ATTN: Tech. Lib.

Director
Defense Communications Agency
ATTN: Code 930, Franklin D. Moore
ATTN: Code 930

Defense Documentation Center
12 cy ATTN: TC

Director
Defense Intelligence Agency
ATTN: DT-1C
ATTN: DT-2, Wpns. & Sys. Div.
ATTN: Tech. Lib.
ATTN: DI-7E
ATTN: DI-7D, Edward O' Farrell

Director
Defense Nuclear Agency
ATTN: DDST
ATTN: STSI, Archives
2 cy ATTN: SPSS
3 cy ATTN: STTL, Tech. Lib.

Director of Defense Research & Engineering
ATTN: DD/S&SS
ATTN: DD/I&SS
ATTN: DD/TWP
ATTN: AD/SW

Commander
Field Command
Defense Nuclear Agency
ATTN: FCTMOF
ATTN: FCPR

Commandant
Industrial College of the Armed Forces
ATTN: Tech. Lib.

Director
Interservice Nuclear Weapons School
ATTN: Tech. Lib.

DEPARTMENT OF DEFENSE (Continued)

Director
Joint Strategic Target Planning Staff, JCS
ATTN: JLTW-2
ATTN: STINFO Library
ATTN: DOXT
ATTN: XPFS

Chief
Livermore Division, Field Command, DNA
ATTN: FCPRL

Commandant
National War College
ATTN: NWCLB-CR

DEPARTMENT OF THE ARMY

Director
Ballistic Missile Defense Advanced Technical Center
ATTN: CRDABH-S
ATTN: CRDABH-X

Program Manager
Ballistic Missile Defense Program Office
ATTN: John Shea

Commander
Ballistic Missile Defense System Command
ATTN: BDMSC-TEN, Noah J. Hurst

Deputy Chief of Staff for Research, Development & Acq.
ATTN: Tech. Lib.

Chief of Engineers
Department of the Army
ATTN: DAEN-MCE-D
ATTN: DAEN-RDM

Deputy Chief of Staff for Ops. & Plans
ATTN: Tech. Lib.
ATTN: Dir. of Chem. & Nuc. Ops.

Commander
Harry Diamond Laboratories
ATTN: DRXDO-NP
ATTN: DRXDO-TI, Tech. Lib.

Commander
Picatinny Arsenal
ATTN: Tech. Lib.

Commander
U.S. Army Armament Command
ATTN: Tech. Lib.

Director
U.S. Army Ballistic Research Laboratories
ATTN: DRXBR-X, Julius J. Meszaros
ATTN: AMXBR-TL-IR, J. H. Keefer
ATTN: W. Taylor
2 cy ATTN: Edward Baicy, Tech. Lib.

Commander
U.S. Army Communications Command
ATTN: Tech. Lib.

DEPARTMENT OF THE ARMY (Continued)

Commander
U.S. Army Electronics Command
ATTN: DRSEL-TL-IR, Edwin T. Hunter

Commander
U.S. Army Engineer Center
ATTN: ATSEN-SY-L

Project Engineer
U.S. Army Engineer Division, Huntsville
ATTN: HNDSE-R, Michael M. Dembo

Division Engineer
U.S. Army Engineer Division, Ohio River
ATTN: Tech. Lib.

Director
U.S. Army Engineer Waterways Experiment Station
ATTN: William Flathau
ATTN: Tech. Lib.
ATTN: Guy Jackson
ATTN: John N. Strange
ATTN: Leo Ingram

Commander
U.S. Army Foreign Science & Technical Center
ATTN: Research & Concepts Branch

Commander
U.S. Army Mat. & Mechanics Research Center
ATTN: Tech. Lib.
ATTN: John Mescall
ATTN: Richard Shea

Commander
U.S. Army Materiel Development & Readiness Command
ATTN: Tech. Lib.
ATTN: DRCDE-D, Lawrence Flynn
2 cy ATTN: DRCRD-BN
ATTN: DRCRD-WN
ATTN: W. H. Hubbard

Commander
U.S. Army Missile Command
ATTN: Tech. Lib.
ATTN: DRSMI-XS, Chief Scientist

Commander
U.S. Army Mobility Equipment R & D Center
ATTN: Tech. Lib.

Commander
U.S. Army Nuclear Agency
ATTN: ATCA-NAW
ATTN: Tech. Lib.

Commandant
U.S. Army War College
ATTN: Library

DEPARTMENT OF THE NAVY

Chief of Naval Material
ATTN: Mat 0323

Chief of Naval Operations
ATTN: OP-985F
ATTN: OP-03EG

DEPARTMENT OF THE NAVY (Continued)

Chief of Naval Research
ATTN: Nicholas Perrone
ATTN: Code 464, Jacob L. Warner
ATTN: Tech. Lib.
ATTN: Code 464, Thomas P. Quinn

Officer-in-Charge
Civil Engineering Laboratory
ATTN: Tech. Lib.
ATTN: R. J. Odello
ATTN: Stan Takahashi

Commander
Naval Electronic Systems Command
ATTN: PME 117-21A

Commander
Naval Facilities Engineering Command
ATTN: Code 04-B
ATTN: Tech. Lib.
ATTN: Code 03-A

Superintendent (Code 1424)
Naval Postgraduate School
ATTN: Code 2124, Tech. Rpts. Librarian

Director
Naval Research Laboratory
ATTN: Code 8440, F. Rosenthal
ATTN: Code 2027, Tech. Lib.

Commander
Naval Sea Systems Command
ATTN: ORD-91313, Library
ATTN: Code 03511

Commander
Naval Ship Engineering Center
ATTN: Tech. Lib.
ATTN: NSEC 6105G

Commander
Naval Ship Research & Development Center
ATTN: Code L42-3, Library

Commander
Naval Ship Research & Development Center
Underwater Explosive Research Division
ATTN: Tech. Lib.

Commander
Naval Surface Weapons Center
ATTN: Code 240, C. J. Aronson
ATTN: Code WA-501, Navy Nuc. Prgms. Off.
ATTN: Code WX-21, Tech. Lib.

Commander
Naval Surface Weapons Center
ATTN: Tech. Lib.

Commander
Naval Undersea Center
ATTN: Tech. Lib.

President
Naval War College
ATTN: Tech. Lib.

DEPARTMENT OF THE NAVY (Continued)

Commander
Naval Weapons Center
ATTN: Code 533, Tech. Lib.

Commanding Officer
Naval Weapons Evaluation Facility
ATTN: R. Hughes
ATTN: Tech. Lib.

Director
Strategic Systems Project Office
ATTN: NSP-43, Tech. Lib.
ATTN: NSP-273
ATTN: NSP-272

DEPARTMENT OF THE AIR FORCE

Commander
ADC/XP
ATTN: XPQDQ
ATTN: XP

AF Geophysics Laboratory, AFSC
ATTN: LWW, Ker C. Thompson
ATTN: SUOL, AFCRL, Research Library

AF Institute of Technology, AU
ATTN: Library, AFIT, Bldg. 640, Area B

AF Weapons Laboratory, AFSC
ATTN: DEV, M. A. Plamondon
ATTN: DEV, Jimmie L. Bratton
ATTN: DE-I
ATTN: DEX
ATTN: Robert Henny
ATTN: Robert Port
ATTN: SUL

Headquarters
Air Force Systems Command
ATTN: DLCAW
ATTN: Tech. Lib.

Commander
Armament Development & Test Center
ATTN: Tech. Lib.
ATTN: ADBRL-2

Commander
ASD
ATTN: Tech. Lib.

Commander
Foreign Technology Division, AFSC
ATTN: TDFBD
ATTN: TDPMG
ATTN: ETET, Capt Richard C. Husemann
ATTN: TD-BTA, Library

HQ USAF/IN
ATTN: IN

HQ USAF/PR
ATTN: PRE

HQ USAF/RD
ATTN: RDQPN
ATTN: RDPM

DEPARTMENT OF THE AIR FORCE (Continued)

Commander
Rome Air Development Center, AFSC
ATTN: EMTLD, Doc. Lib.
ATTN: EMREC, R. W. Mair

SAMSO/DE
ATTN: DEB

SAMSO/DY
ATTN: DYS

SAMSO/MN
ATTN: MMH
ATTN: MNNH

SAMSO/XR
ATTN: XRTB

Commander in Chief
Strategic Air Command
ATTN: NRI-STINFO Library
ATTN: XPFS

ENERGY RESEARCH & DEVELOPMENT ADMINISTRATION

Division of Military Application
U.S. Energy Research & Development Administration
ATTN: Doc. Con. for Test Office

University of California
Lawrence Livermore Laboratory
ATTN: D. M. Norris, L-90
ATTN: Ted Butkovich, L-200
ATTN: J. R. Hearst, L-205
ATTN: Jack Kahn, L-7
ATTN: J. Carothers, L-7
ATTN: Tech. Info., Dept. L-3
ATTN: Robert Schock, L-437
ATTN: Larry W. Woodruff, L-96
ATTN: Richard G. Dong, L-90

Los Alamos Scientific Laboratory
ATTN: Doc. Con. for G. R. Spillman
ATTN: Doc. Con. for Al Davis
ATTN: Doc. Con. for Reports Lib.

Sandia Laboratories
Livermore Laboratory
ATTN: Doc. Con. for Tech. Lib.

Sandia Laboratories
ATTN: Doc. Con. for A. J. Chaban
ATTN: Doc. Con. for M. L. Merritt
ATTN: Doc. Con. for Luke J. Vortman
ATTN: Doc. Con. for 3141, Sandia Rpt. Coll.
ATTN: Doc. Con. for W. Roherty
ATTN: L. Hill

U.S. Energy Research & Development Administration
Albuquerque Operations Office
ATTN: Doc. Con. for Tech. Lib.

U.S. Energy Research & Development Administration
Division of Headquarters Services
ATTN: Doc. Con. for Class. Tech. Lib.

U.S. Energy Research & Development Administration
Nevada Operations Office
ATTN: Doc. Con. for Tech. Lib.

ENERGY RESEARCH & DEVELOPMENT ADMINISTRATION (Continued)

Union Carbide Corporation
ATTN: Doc. Con. for Tech. Lib.
ATTN: Civil Def. Res. Proj.

OTHER GOVERNMENT AGENCIES

Bureau of Mines
ATTN: Tech. Lib.

Central Intelligence Agency
ATTN: RD/SI, Rm. 5G48, Hdq. Bldg. for NED/OSI-5G48, Hdqs.

Department of the Interior
Bureau of Mines
ATTN: Tech. Lib.

Department of the Interior
Bureau of Mines
ATTN: James J. Scott

Department of the Interior
U.S. Geological Survey
ATTN: J. H. Healy
ATTN: Cecil B. Raleigh

DEPARTMENT OF DEFENSE CONTRACTORS

Aerospace Corporation
ATTN: Prem N. Mathur
2 cy ATTN: Tech. Info. Services

Agbabian Associates
ATTN: M. Agbabian

Analytic Services, Inc.
ATTN: George Hesselbacher

Applied Theory, Inc.
2 cy ATTN: John G. Trulio

Artec Associates, Inc.
ATTN: Steven Gill

Avco Research & Systems Group
ATTN: Research Library, A-830, Rm. 7201

Battelle Memorial Institute
ATTN: Tech. Lib.
ATTN: R. W. Klingesmith

The BDM Corporation
ATTN: Tech. Lib.
ATTN: A. Lavagnino

The BDM Corporation
ATTN: Richard Hensley

The Boeing Company
ATTN: Aerospace Library
ATTN: R. H. Carlson

Brown Engineering Company, Inc.
ATTN: Manu Patel

California Institute of Technology
ATTN: Thomas J. Ahrens

DEPARTMENT OF DEFENSE CONTRACTORS (Continued)

California Research & Technology, Inc.
ATTN: Ken Kreyenhagen
ATTN: Tech. Lib.

University of California
ATTN: G. Sackman

Calspan Corporation
ATTN: Tech. Lib.

Civil/Nuclear Systems Corp.
ATTN: Robert Crawford

University of Dayton
ATTN: Hallock F. Swift

University of Denver
Colorado Seminary
ATTN: Sec. Officer for J. Wisotski
ATTN: Sec. Officer for Tech. Lib.

EG&G, Inc.
Albuquerque Division
ATTN: Tech. Lib.

The Franklin Institute
ATTN: Zenons Zudans

General American Transportation Corp.
General American Research Division
ATTN: G. L. Neidhardt

General Electric Company
Space Division
ATTN: M. H. Bortner, Space Sci. Lab.

General Electric Company
Re-Entry & Environmental Systems Division
ATTN: Arthur L. Ross

General Electric Company
TEMPO-Center for Advanced Studies
ATTN: DASIAC

General Research Corporation
ATTN: Benjamin Alexander

IIT Research Institute
ATTN: R. E. Welch
ATTN: Milton R. Johnson
ATTN: Tech. Lib.

Institute for Defense Analyses
ATTN: IDA, Librarian, Ruth S. Smith

J. H. Wiggins Co., Inc.
ATTN: John Collins

Kaman Avidyne
Division of Kaman Sciences Corp.
ATTN: E. S. Criscione
ATTN: Norman P. Hobbs
ATTN: Tech. Lib.

Kaman Sciences Corporation
ATTN: Paul A. Ellis
ATTN: Frank H. Shelton
ATTN: Library

DEPARTMENT OF DEFENSE CONTRACTORS (Continued)

Lockheed Missiles & Space Co., Inc.
ATTN: Tech. Lib.

Lovelace Foundation for Medical Education & Research
ATTN: Tech. Lib.
ATTN: Asst. Dir. of Res., Robert K. Jones

Martin Marietta Aerospace
Orlando Division
ATTN: G. Fotieo

McDonnell Douglas Corporation
ATTN: Robert W. Halprin

Merritt Cases, Incorporated
ATTN: Tech. Lib.
ATTN: J. L. Merritt

Meteorology Research, Inc.
ATTN: William D. Green

The Mitre Corporation
ATTN: Library

Nathan M. Newmark
Consulting Engineering Services
ATTN: Nathan M. Newmark

Pacifica Technology
ATTN: G. Kent
ATTN: R. Bjork

Physics International Company
ATTN: Doc. Con. for Tech. Lib.
ATTN: Doc. Con. for E. T. Moore
ATTN: Doc. Con. for Coye Vincent
ATTN: Doc. Con. for Fred M. Sauer
ATTN: Doc. Con. for Robert Swift
ATTN: Doc. Con. for Larry A. Behrmann
ATTN: Doc. Con. for Dennis Orphal
ATTN: Doc. Con. for Charles Godfrey

R & D Associates
ATTN: Tech. Lib.
ATTN: J. G. Lewis
ATTN: Jerry Carpenter
ATTN: Henry Cooper
ATTN: William B. Wright, Jr.
ATTN: Bruce Hartenbaum
ATTN: Cyrus P. Knowles
ATTN: Albert L. Latter
ATTN: Sheldon Schuster
ATTN: Harold L. Brode

The Rand Corporation
ATTN: C. C. Mow

Science Applications, Inc.
ATTN: David Bernstein
ATTN: D. E. Maxwell

Science Applications, Inc.
ATTN: R. Seebaugh
ATTN: John Mansfield

Science Applications, Inc.
ATTN: Tech. Lib.
ATTN: Michael McKay

DEPARTMENT OF DEFENSE CONTRACTORS (Continued)

Science Applications, Inc.
ATTN: R. A. Shunk

Southwest Research Institute
ATTN: Wilfred E. Baker
ATTN: A. B. Wenzel

Stanford Research Institute
ATTN: Carl Peterson
ATTN: George R. Abrahamson

Systems, Science & Software, Inc.
ATTN: Thomas D. Riney
ATTN: Ted Cherry
ATTN: Donald R. Grine
ATTN: Tech. Lib.

Terra Tek, Inc.
ATTN: A. H. Jones
ATTN: Tech. Lib.
ATTN: Sidney Green

Tetra Tech, Inc.
ATTN: Tech. Lib.
ATTN: Li-San Hwang

TRW Systems Group
ATTN: Norm Lipner
ATTN: Benjamin Sussholtz
ATTN: Jack Farrell
ATTN: William Rowan
ATTN: Tech. Info. Ctr., S-1930
ATTN: Paul Lieberman
ATTN: Pravin Bhutta

TRW Systems Group
San Bernardino Operations
ATTN: Gregory D. Hulcher

Universal Analytics, Inc.
ATTN: E. I. Field

URS Research Company
ATTN: Tech. Lib.
ATTN: Ruth Schneider

The Eric H. Wang
Civil Engineering Research Facility
ATTN: Neal Baum
ATTN: Larry Bickle

Washington State University
Administrative Office
ATTN: Arthur Miles Hohorf for George Duval

Weidlinger Assoc. Consulting Engineers
ATTN: Melvin L. Baron
ATTN: Joseph P. Wright
ATTN: John L. Baylor

Westinghouse Electric Company
Marine Division
ATTN: W. A. Volz